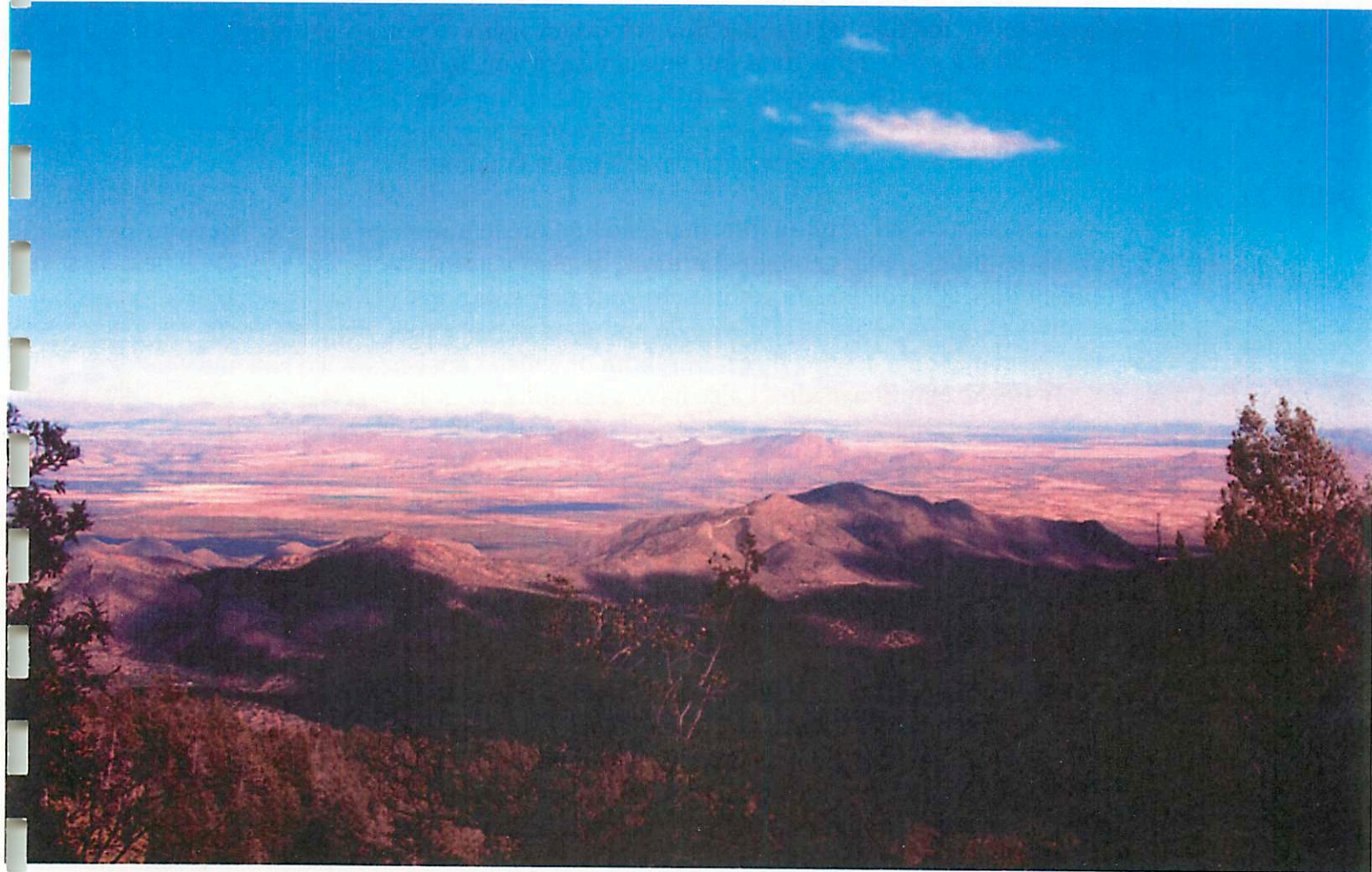


LIBRARY  
LUNAR & PLANETARY LAB

# Field and Presentation Guide: Chiricahua Mountains, Volcanoes of San Bernardino Valley, and Willcox Playa

In which we discuss plans of our adventures.



November 20-22, 2009

PTY5 594A: Planetary Geology Field Practicum

Or

“What planetary scientists do when you let them out of their offices.”

QE40  
.P63  
C451  
2009

Dear Readers:

I got stuck with this job because I got into a debate with Dave Choi about the relative ease of photocopying. That was dumb. But nevertheless, I had resigned myself to defending my superior copy skills and do the job right. I used to work at a copy center where I was copy queen. It turns out, however, that I seem to have lost my copy prowess. Or else Dave turned the LPL copier against me, because last time I tried to make copies it suddenly decided (four times) of its own volition that the front door was open, and would refuse to continue until I had closed it, which actually consisted of me turning the machine off and on again. If you are reading this I have clearly succeeded this time, but I would warn you, fellow students, to be wary of those machines. They may be plotting and scheming with the printers behind our backs. And I wouldn't let Dave anywhere near anything electronic, just in case. For now, I will let the debate rest: Dave 1, Jamie 0, Copier 4.

At any rate, this is intended to be an informal field and presentation guide. I will not spend time here talking about geology; there will be plenty of that along the way. I do hope the guide will be of use. In addition to your presentations, I have included some basic hwy maps for those of you who do not excel at being followers. There is a loose schedule and some driving directions, both of which I am certain we will not follow, even if the attempt be made. I also have a section that is an overview of the sites, with some images, graphs, maps, etc. In retrospect, I really didn't need to add the images, since we will in fact be there to see it ourselves. But just in case we leave one of you behind, you'll at least have a picture as a memento of what you missed out on while everyone else was busy having fun without you. Hopefully we can manage to come home without any tents catching fire, visits from overly "friendly" woodland creatures (or illegal immigrants), dismantled vehicles, or missing organs.

I am very excited about this trip. It will be my first field trip with LPL, and my first camping trip in Arizona since I was a kid. I really love camping, and do so any chance I get. I only hope you all being there won't ruin it for me. I jest, of course. I am really looking forward to some bonding, some laughing, some science, and the great outdoors. I have no doubt that with our fearless leader and insatiable curiosity this will be a great experience.

Without further ado, onward, friends, to adventure!

-Jamie Molaro

Editor in Chief, First-Year, Former Copy Queen, and Aspiring Scientist  
LPL Field Trip, Fall 2009

## Table of Contents

Trip Itinerary	2
Basic Driving Maps	3
Overview of Sites and Topics with Images	7
Presentations:	
Day 1	
Juan Lora – Texas Canyon and spheroidal weathering	10
Colin Dundas – Playa desiccation cracks	13
Christopher Dietl – Playas and water history in the Southwest since the last ice-age	17
Doug Archer – Evaporate formation	21
Ingrid Spitale – Clay Dunes	25
Jamie Molaro – Chiricahua Hoodoos	28
Tom Schad – Turkey creek eruption: Stabilized dunes	31
Day 2	
Catherine Elder – Plate tectonics and basin and range formation	34
Shane Byrne – History of San Bernardino field	38
Patricio Bercerra – Formation of maar craters	40
Eve Berger – Mantle nodules	44
David Choi – 1887 Earthquake	48
Peng Sun – East Chiricahuas Alluvial fans	52
Kat Volk – Indian History	54
Day 3	
Serina Diniega – Clovis ‘Impact’ Layer	56

## Itinerary (sort of)

### Day 1:

- 7 am Meet at LPL loading dock  
8 am Get on the road! Head East on I-10 for ~50 miles to Texas Canyon.  
9 am Arrive at Texas Canyon.  
11 am Head East on I-10 for ~16 miles. Take exit 331 onto 191 S, drive a few miles, pull over at Wilcox Playa. Map B  
11:20 am Arrive at Wilcox Playa. Eat Lunch.  
12:00 pm Return to I-10, heading East for ~5 miles. Take exit 336 towards Willcox. Merge onto S Haskell Ave. Turn right at 186 E/E Maley St. Continue for ~30 miles and turn left onto 181 E.  
1:30 pm Arrive in at the Chiricahua Mountains. Stop at whatever sites Shane says.  
5ish Find a place to camp for the night.

### Day 2:

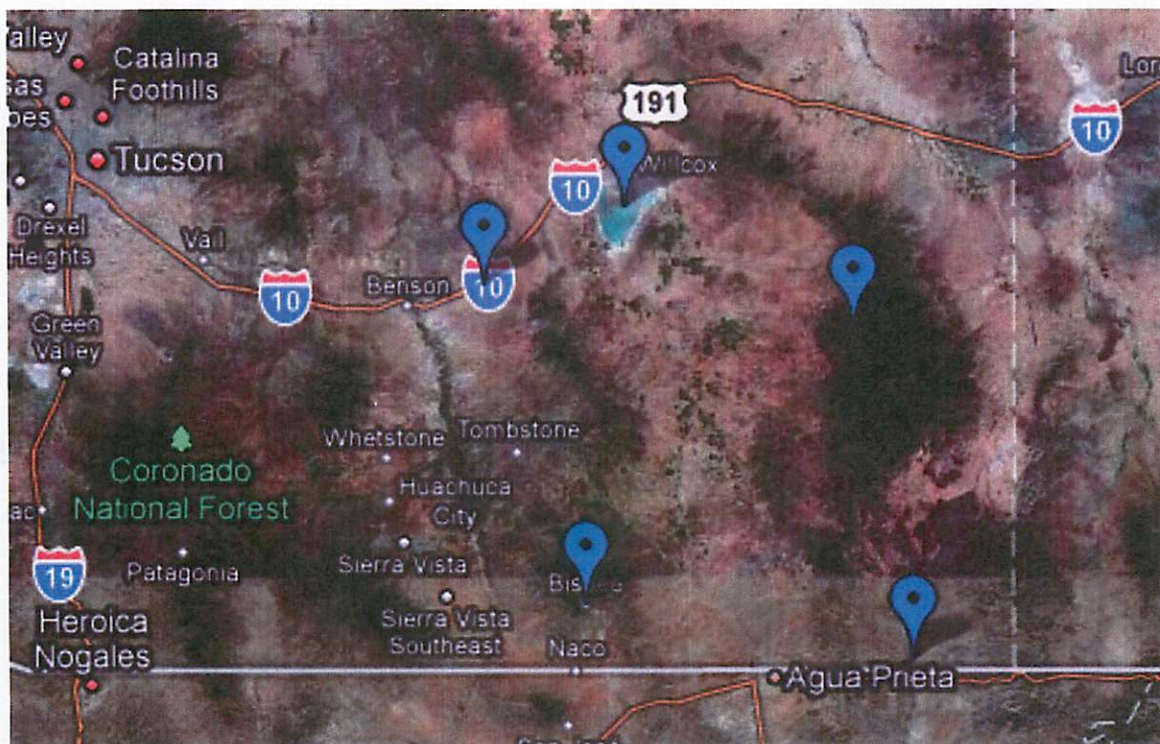
- 8 am Break Camp. Head W on 181 for (depending on where we camp) maybe 20-30 miles. Turn left at 191 S, and drive for 40 miles. Turn left at 80 E and continue up into San Bernadino Valley.  
10 am Arrive in vicinity of the valley, go where adventure takes us! We'll visit Paramore Crater, Cochise Crater, and Sotse Crater, as well as a few places that are unnamed.  
5ish Find a place to camp for the night.

### Day 3:

- 8 am Break Camp. Head west on 80 out of the valley. The drive to Bisbee is about 35 miles from the west edge of the valley.  
10 am Arrive in Bisbee. Invade the town. Early lunch?  
12 pm Head west on 80 (going north) and drive for ~45 miles. When we get to Benson, we essentially have to make a U-turn to get onto I-10 E. Turn left at San Pedro Drive, and immediately (really) left at E 4<sup>th</sup> St/I-10 BUS E. Continue for a mile or two. Turn left at N Pomerene and drive for ~4 miles, then turn right onto N Cascabel Rd. This leads into the San Pedro Valley, and where Murray Springs is, somewhere.  
2 pm Arrive at Murray Springs.  
3 pm Return to Benson, and head W on I-10, toward home.  
4 pm Home again, phew!

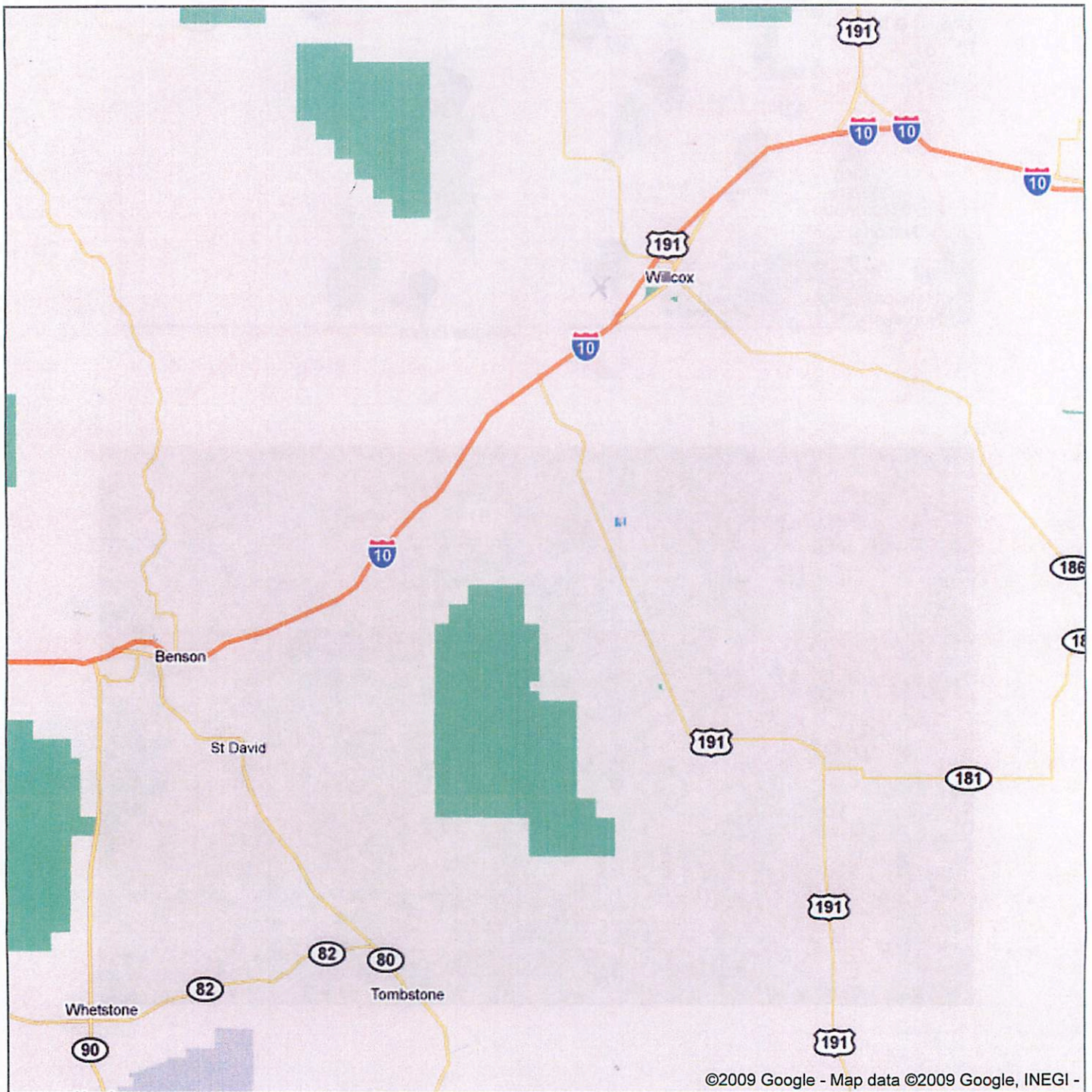

## General Map (Map A)

Sites (from left to right, top to bottom) are: Texas Canyon, Wilcox Playa, Chiricahua Mountains, Bisbee, and the San Bernadino Valley



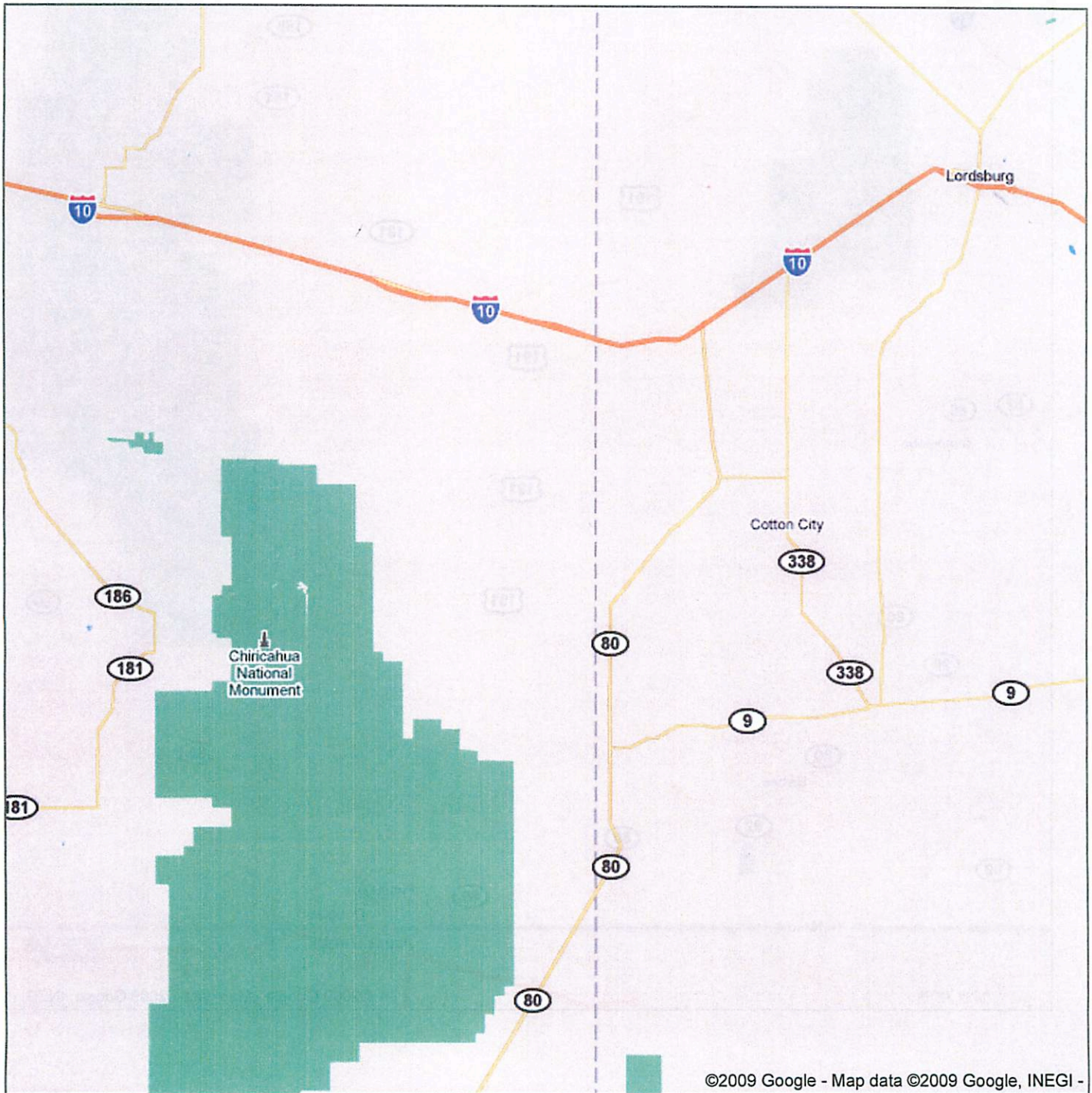
Google maps Address Arizona

Get Google Maps on your phone  
Text the word "GMAPS" to 466453



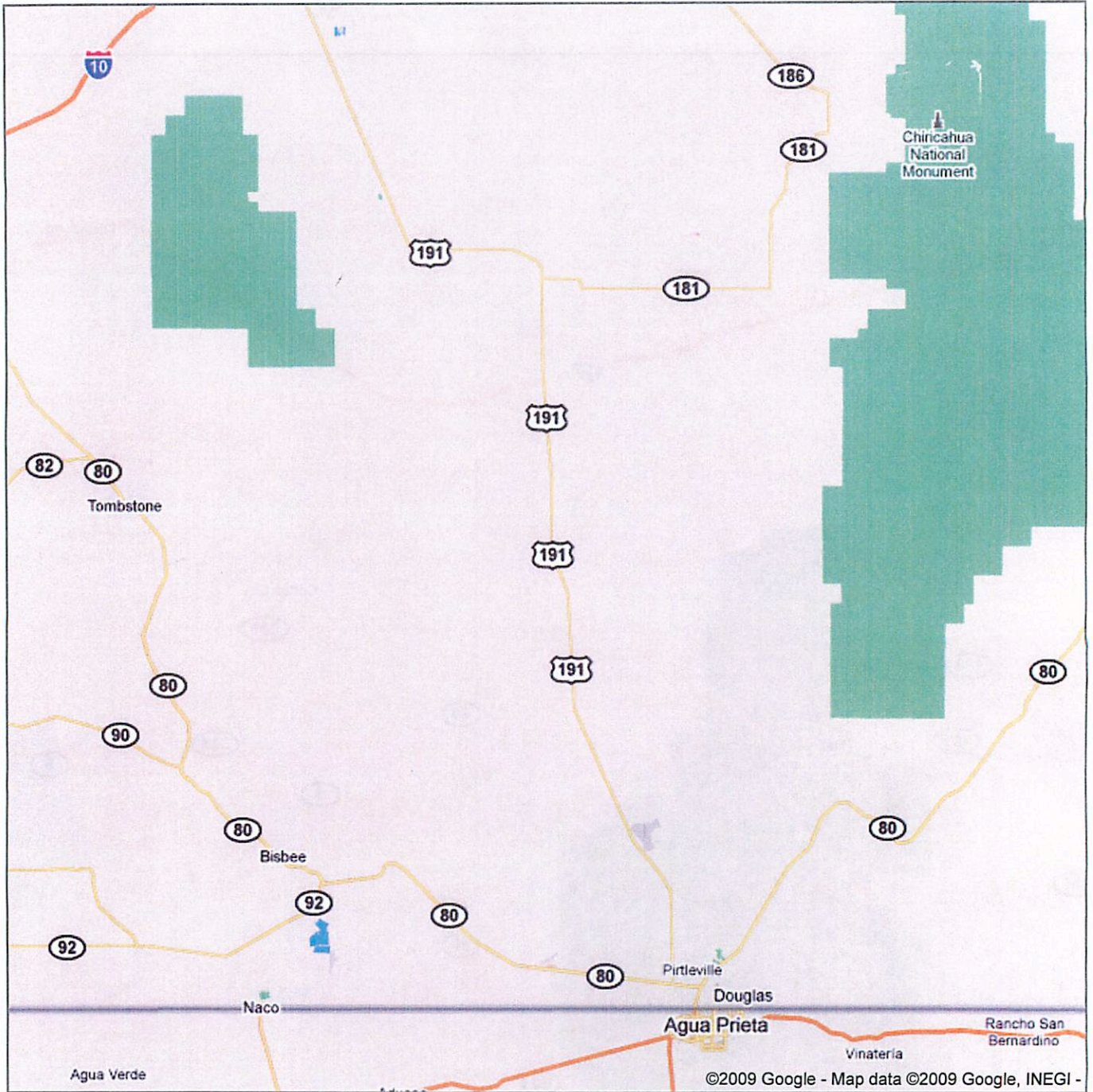

Google maps Address Arizona

Get Google Maps on your phone  
Text the word "GMAPS" to 466453



Google maps Address Arizona

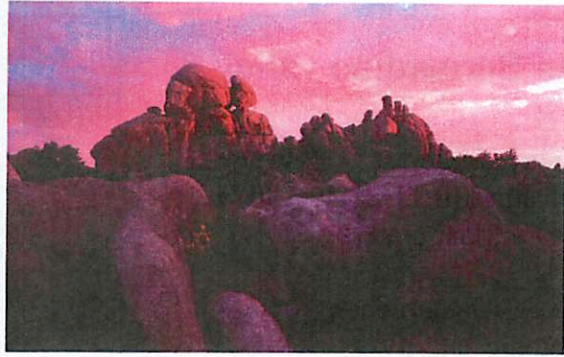
Get Google Maps on your phone  
Text the word "GMAPS" to 466453





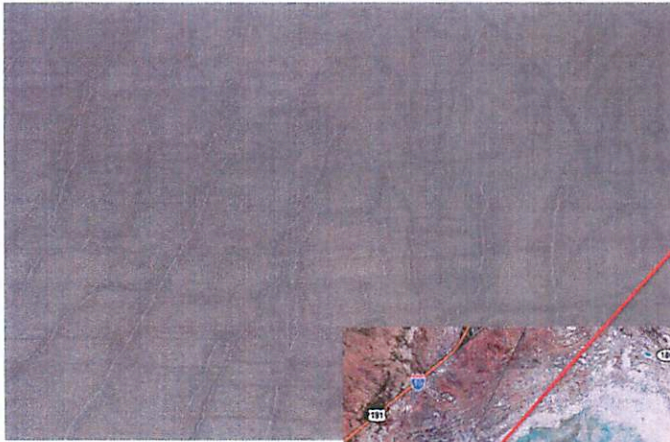
## Texas Canyon

Topics of interest:  
History (stagecoach route,  
Texan ranchers), granite  
boulders, saloon, spheroidal  
weathering



## Chiricahua Mountains

Topics of interest:  
Hoodoos, Dunes, lots of  
other geology



## Wilcox Playa

Topics of interest:  
polygonal patterns, clay dunes,  
desiccation cracks



# San Bernardino valley

Topics of interest:

Volcanics (0.3 – 3 Myr old)

Maar craters

Tuff rings

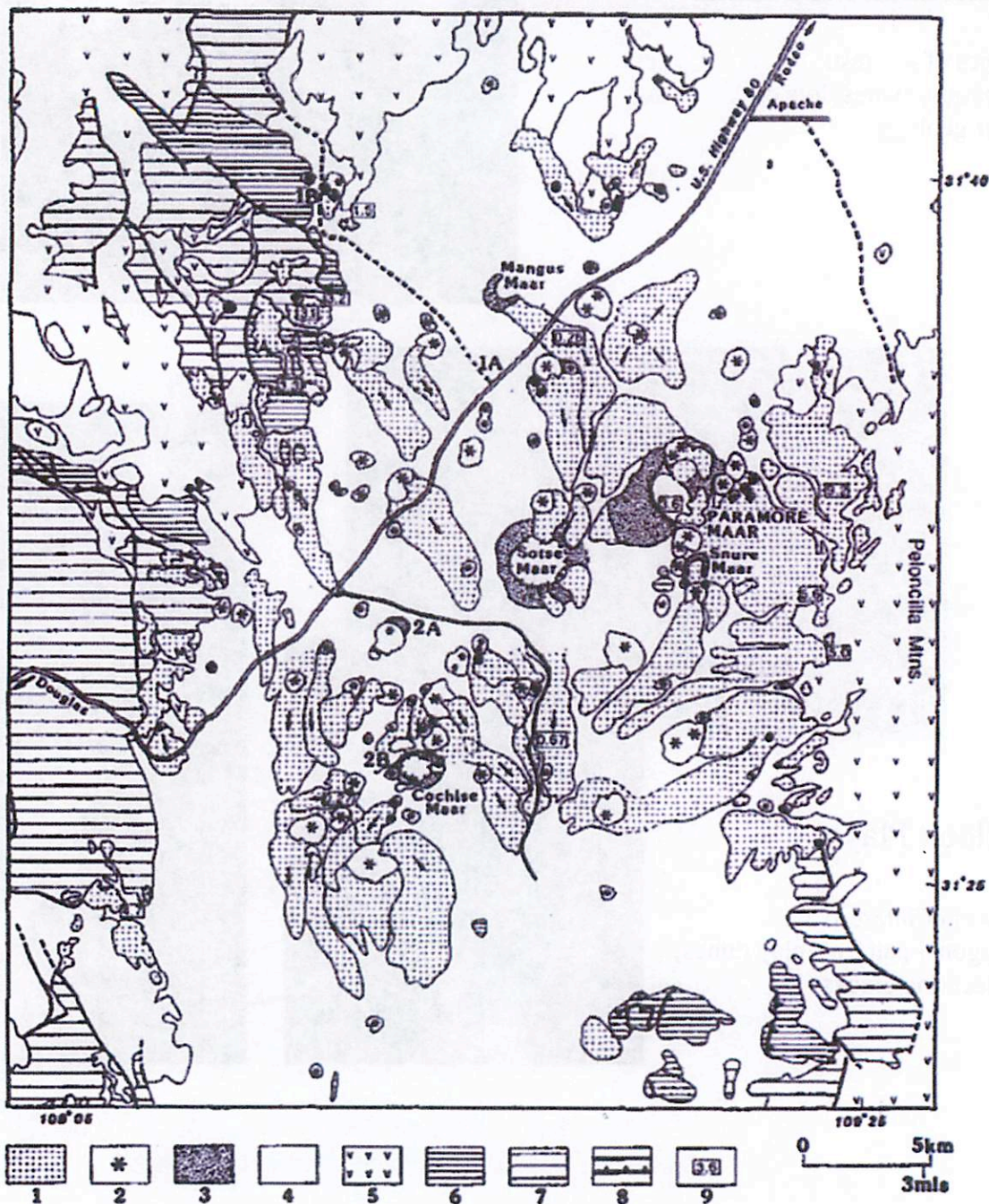
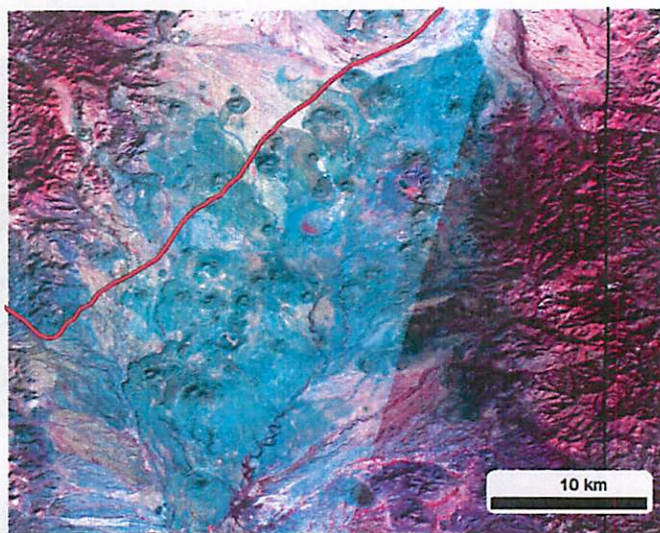
Cinder cones

Tectonic activity

Recent large earthquake

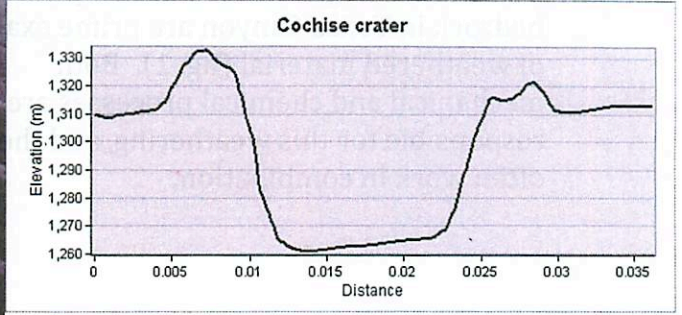
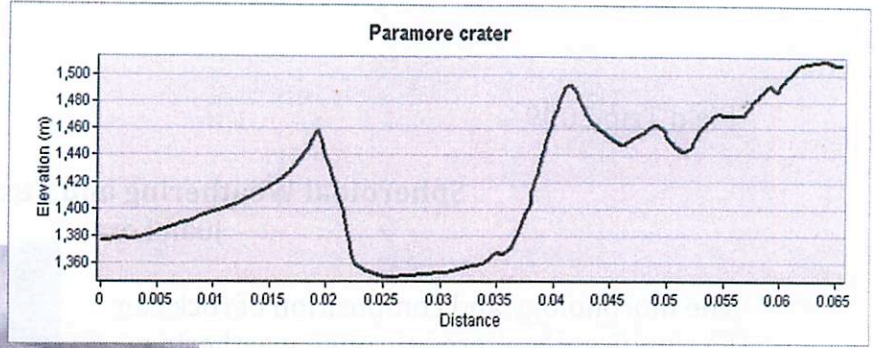
Basin & range control

Basalt Flows in IR →

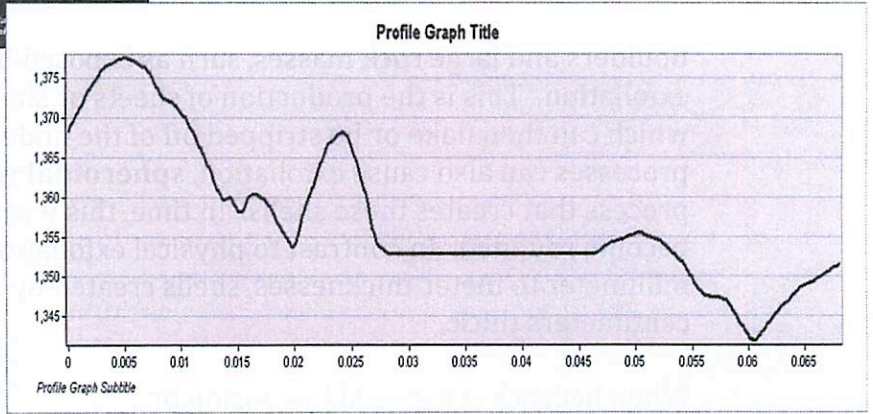




Paramore Crater & Sun Berradino Valley  
Aerial view north  
Photograph

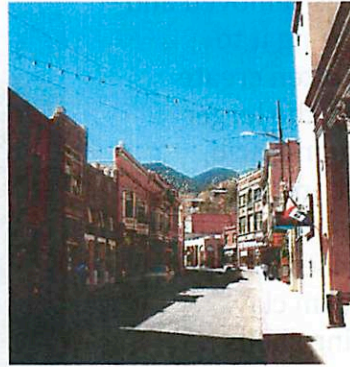


Paramore Crater ^  
Sotse Maar →



## Bisbee

Topics of Interest:  
The town!



## Murray Springs

Topics of Interest:  
Desert Spring  
Stratigraphic Records  
Paleoindian Sites



## Spheroidal Weathering and Texas Canyon

Juan Lora

The morphology and composition of rock can be significantly altered through weathering processes. Large boulders and exposed bedrock in Texas Canyon are prime examples of weathered material (fig. 1). Both mechanical and chemical processes are responsible for this weathering, and the two often work in combination.

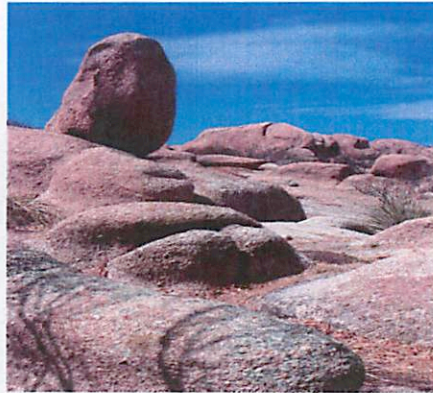


Figure 1: Typical rock formations in Texas Canyon

Boulders and large rock masses, such as exposed bedrock, are readily susceptible to exfoliation. This is the production of sheets or shells by weathering processes, which can then flake or be stripped off of the underlying surface. Although physical processes can also cause exfoliation, **spheroidal weathering** is the chemical process that creates these shells. In time, this weathering can cause rocks to become rounded. In contrast to physical exfoliation, which creates sheets of millimeter to meter thicknesses, shells created by spheroidal weathering are usually centimeters thick.

When bedrock is exposed by erosion or uplift, the overlying pressure is removed and rock can expand laterally, causing it to fracture. The resulting joints often create sharp-edged structures within the larger formation (fig. 2). Weak carbonic acid, formed by rainwater and carbon dioxide, is then able to run through these cracks. Even slightly acidic water decomposes feldspar minerals within the rock to form clays, thereby creating the exfoliating shells characteristic of spheroidal weathering (see fig. 3).

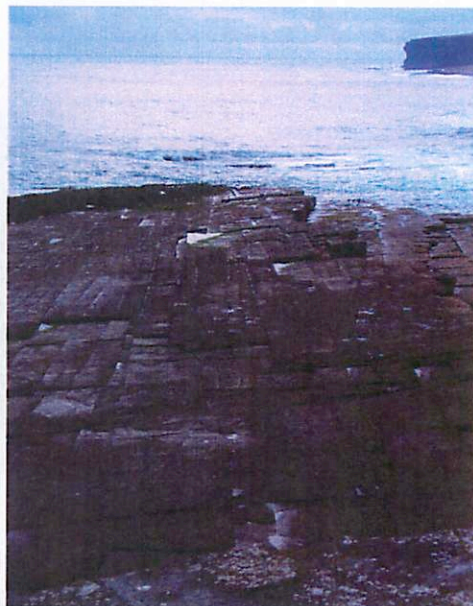


Figure 2: Joint sets at St Mary's Chapel, Caithness, Scotland

Structures with cornered edges, such as recently fractured formations, offer a higher surface area for the running water, and so are more quickly decomposed. They therefore become rounded, and over time the structure becomes more spherical in shape (fig 3). The rate of weathering is then uniform over the available surface area, such that the inner layers of the onion-like concentric shells of decomposed rock are increasingly spherical.

Spheroidal weathering is most common in uniform, hard rocks that are well jointed. Examples of these are granite, dolerite and basalt. Texas Canyon is known for its giant granite boulders, and is thus provides many examples of spheroidal weathering. Similarly, spheroidal weathering may occur on other planets where rock and acidic water can come in contact with each other. On Mars, basaltic formations are commonplace, and there is ample evidence of ancient and (maybe) present-day water flows.

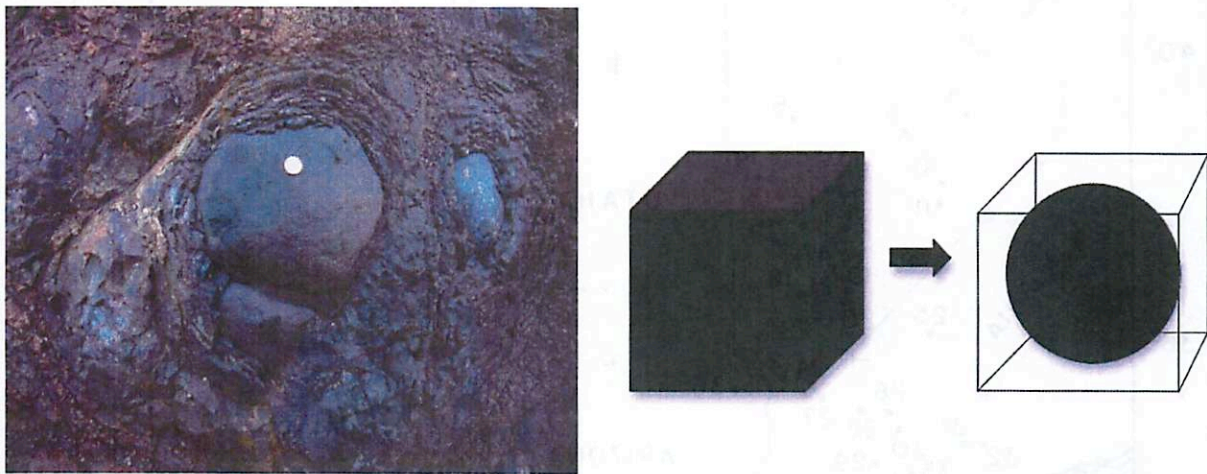


Figure 3: Spheroidal weathering pattern (left) and the geometry of spheroidal weathering (right)

#### References:

Bates, R.L., & Jackson, J.J. Dictionary of Geological Terms. 3<sup>rd</sup> Ed. Random House: New York, 1984.

Flint, R.F. & Skinner, B.J. Physical Geology. 2<sup>nd</sup> Ed. Wiley: New York, 1977.

Ollier, C.D. "Causes of Spheroidal Weathering." *Earth-Sci. Rev.*, 1971. V7. 127-141.  
[http://en.wikipedia.org/wiki/Texas\\_Canyon](http://en.wikipedia.org/wiki/Texas_Canyon)

#### Images

[http://en.wikipedia.org/wiki/File:Texas\\_canyon\\_az.jpg](http://en.wikipedia.org/wiki/File:Texas_canyon_az.jpg)

[http://en.wikipedia.org/wiki/File:Joints\\_Caithness.JPG](http://en.wikipedia.org/wiki/File:Joints_Caithness.JPG)

[http://nvcc.edu/home/cbentley/geoblog/uploaded\\_images/onion-774600.jpg](http://nvcc.edu/home/cbentley/geoblog/uploaded_images/onion-774600.jpg)

# Giant Desiccation Polygons: Potholes on Nature's Racetracks

Colin Dundas

## Definition

**Giant desiccation cracks** are large-scale fissures formed in sediments (typically clay-rich, such as many playas in the western United States). **Giant desiccation polygons** are polygonal patterns formed by giant desiccation cracks.

## Locations

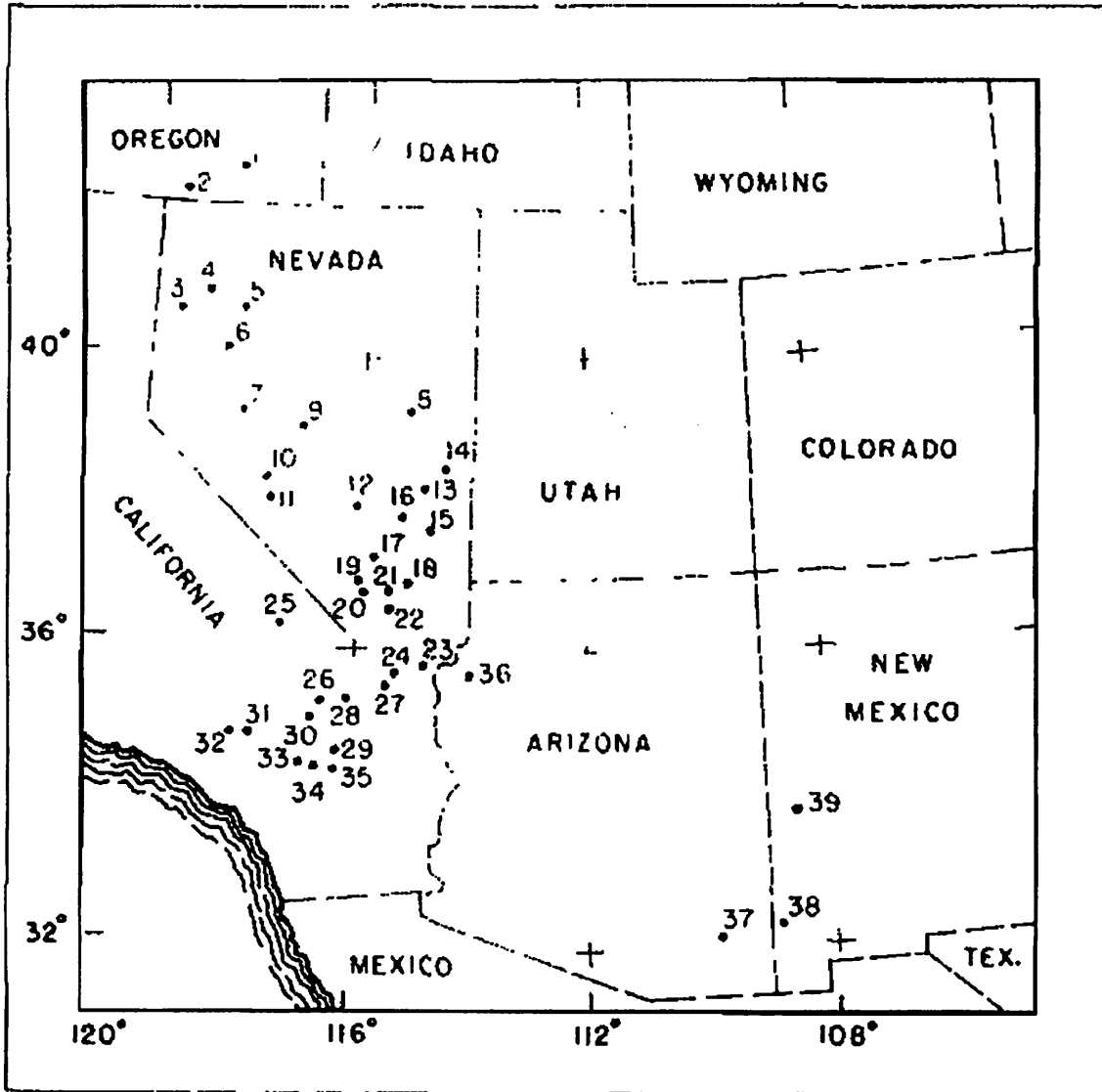


**Figure 1:** Giant desiccation polygon localities reported by Neal et al. (1968). They are generally reported on the surfaces of playas with desiccated surfaces and tens of meters of clay- and silt-rich sediments. Playas with polygons usually have hard, dry surfaces with abundant sheet silicates; other playas have “puffy” surfaces with significant amounts of salt, associated with surface wetting and saturation. No. 37 is Willcox Playa.

## Morphology

Giant desiccation cracks are tens to hundreds of meters long and may be more than 5 m deep when recently opened. In some cases, a slight “lip” is reported at the fissure, standing a few cm above the polygon center.



**Figure 2:** Left: recent desiccation crack on Panamint Playa in California, with person for scale. Below: infilled fissure elsewhere on the playa, now visible only as an albedo stripe. (Figures from Messina et al., 2005).



Messina et al. (2005) described an age progression which illustrates fissure development. New cracks are deep and sharp-edged. Over time, they fill in by slumping and trapping sediment, which eventually allows vegetation to develop. Older fissures may invert and become ridges, before finally being reduced to linear albedo features. The lifespan of a fissure is at least several decades (Messina et al., 2005).

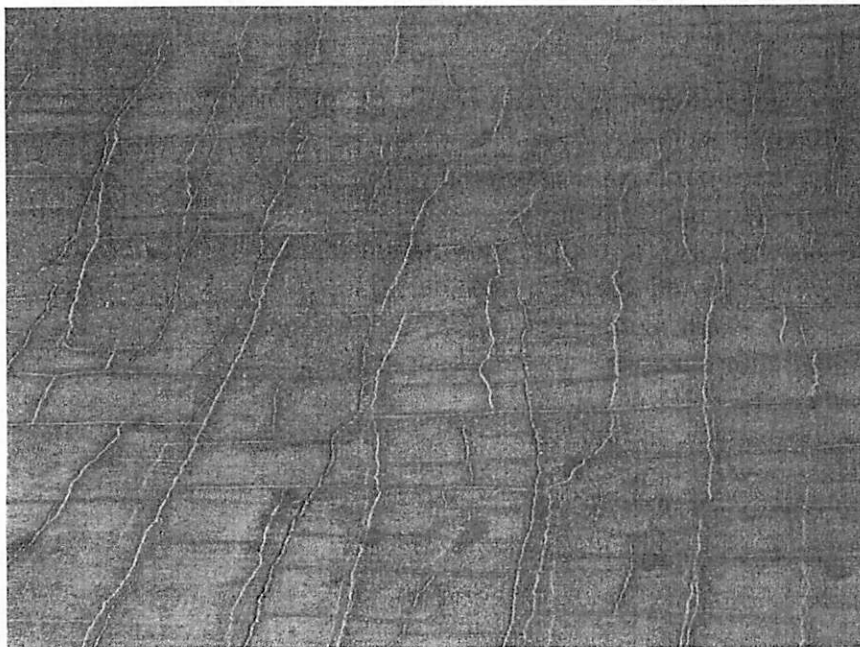


**Figure 3:** Polygons on the eastern side of Willcox Playa. Note rectilinear grid pattern, dark stripes around light fissures, and apparently several generations of fissures. (Image: Joe Spitale/Shane Byrne?) These polygons are unvegetated, while those on the western part of the playa are vegetated and show less rectilinear patterns in some cases.

## **Formation Process**

The formation process is described by Neal et al. (1968), although the basic ideas were noted by earlier references cited there. Giant desiccation cracks form due to long-term water loss and recession of the water table. Clay-rich soils change their volume significantly when they lose water. As they dry, stress builds up, and eventually they crack to relieve the stress. The clay layer must be thick enough to develop substantial stress, and the water table must recede fast enough that this stress cannot be relieved by creep. Cracks generally originate at some depth, not at the surface. They then propagate upwards and downwards, eventually breaching the surface. Somewhat paradoxically, new desiccation cracks often open just after rain or flooding, which softens the surface layer and causes collapse (Messina et al., 2005). Fissures may lengthen over time (Messina et al., 2005).

What causes these cracks to form polygonal patterns? An orthogonal grid pattern is easy to understand. The orientation of initial fissures may be set by any anisotropy in the stress field; for instance, a slope in the surface of the water table (Neal et al., 1968). Once a fissure is formed, it relieves the stress in one direction for some distance, but other cracks are likely to form in parallel due to the same anisotropy. Perpendicular cracks will form because stresses in the orthogonal dimension must also be relieved, and an orthogonal intersection is likely since the crack becomes a free surface. Non-grid patterns are likely in the absence of any source of anisotropy, but the same boundary effect may still cause orthogonal intersections.

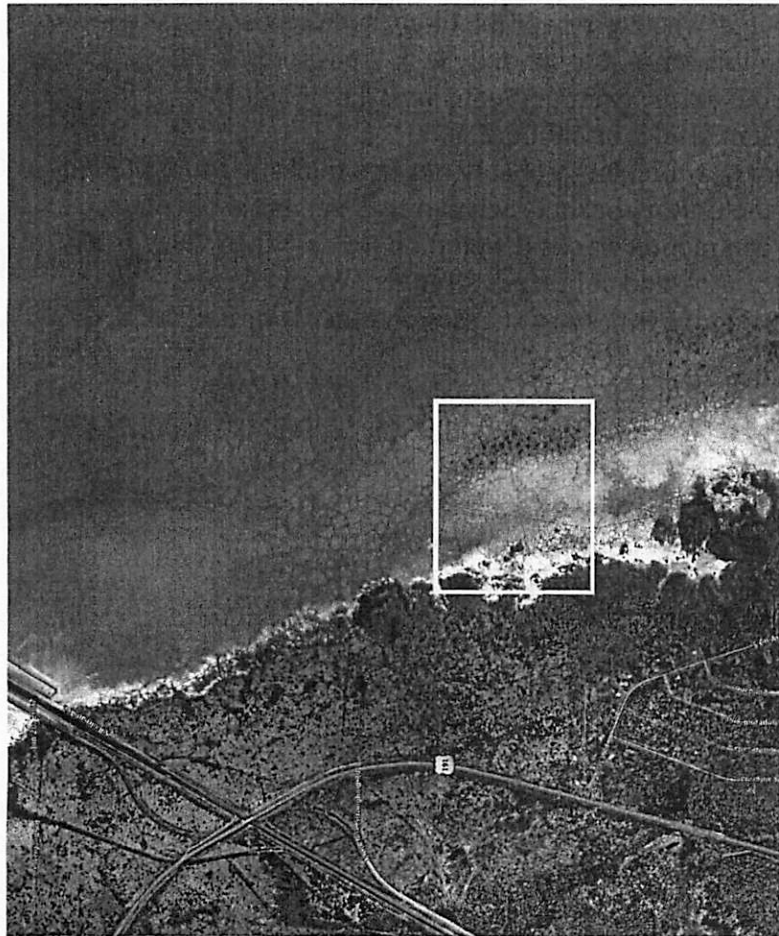
## **Willcox Playa—What to Look For**

Aerial photos indicate that Willcox Playa has abundant large polygons formed by desiccation cracks. These form a fairly orthogonal grid in the eastern part of the playa, and are more isotropic in the western part. There are also cross-cutting cracks, indicating multiple generations of activity. Cracks in the western part of the playa also frequently appear vegetated, but this doesn't appear common in the grid-like polygons to the east. In aerial photos, the cracks often have few-meter-wide swaths on either side, which may appear bright or dark. Neal et al. (1968) noted that Willcox Playa has "oriented orthogonal" and "irregular random orthogonal" polygons, ranging from fresh to albedo-only (but do not note vegetated fissures), and report a scale of 15-30 m. This description mostly applies today as well.

What to look for:

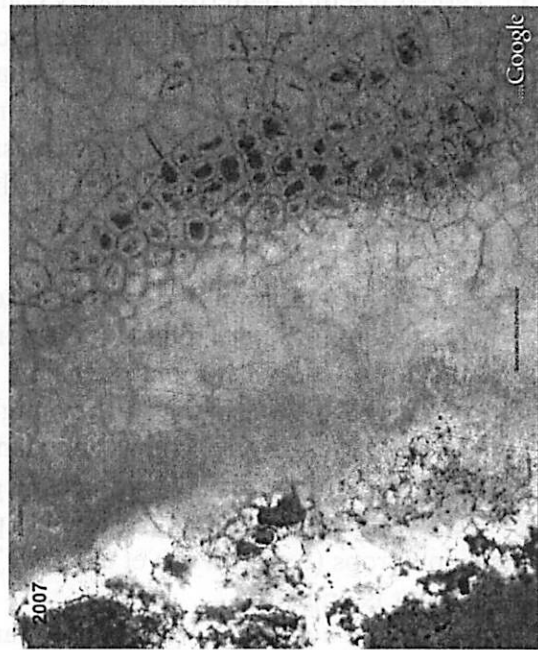
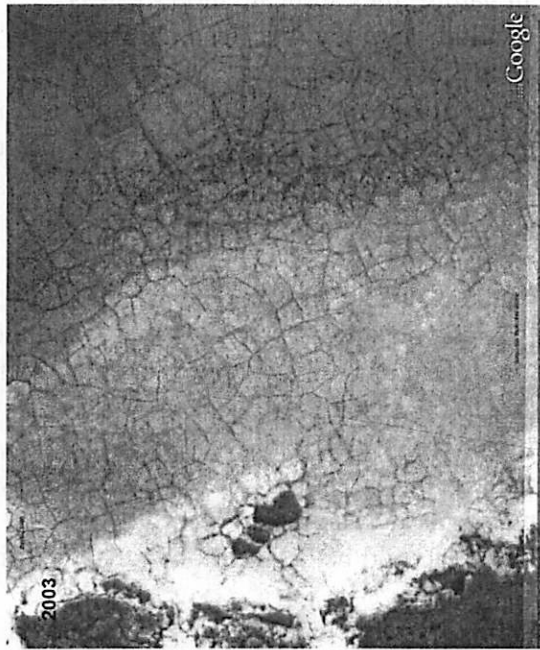
- Can we distinguish different generations of polygon crack at ground level? (Are older cracks more completely filled?)
- If we can dig a trench, what is the nature of the material filling the cracks? (Speculatively, maybe the western polygons are vegetated because they fill in with non-playa material, while the eastern polygons tend to fill with loose material from the playa surface. Is this consistent with the wind direction from clay dunes?)
- What causes the bright or dark swaths around the cracks? (Hypothesis: microrelief causes slightly different hydration states, leading to albedo differences.) Can we see these differences at ground level?
- What are the freshest cracks that we can find? Aerial photos show some examples with definite relief—the troughs show topographic shading. Please do not discover a very fresh example by driving into it, especially if the width is greater than a van tire.





Are the polygons changing? Polygon patterns look different between 2003 and 2007 in Google Earth imagery. (Note upper right corner). However, at least some changes are probably due to different lighting, soil moisture, etc.

The apparent changes in polygon pattern are so large that they actually make me skeptical...



Images credit Google Earth

## Other Polygonal Textures

Polygonal fracture patterns are fairly common in nature; they indicate more-or-less isotropic stress patterns, generally due to contraction. In addition to giant desiccation cracks, polygons of geologic interest can develop in small-scale surficial mud cracks, cooling basalt or other igneous rock (columnar jointing, etc.), permafrost (Lachenbruch, 1962; thermal contraction polygons, with many morphologies), evaporite salts (e.g. Tucker, 1981) or jointed rocks (Pollard and Aydin, 1988; tectonic joints tend to be rectilinear).

## Polygons on Other Planets

Polygonal patterns are found in several settings on the surface of Mars. Giant polygons, far larger than any on Earth, are found on the northern plains; these were proposed to be tectonic features (graben) formed by isotropic extension, since no other mechanism should operate on this scale (Pechmann, 1980). Alternatively, they might be due to compaction of wet sediments (McGill and Hills, 1992). Mars also has abundant thermal contraction cracks (e.g. Mellon et al., 2008) and polygonally textured lava surfaces (e.g. Keszthelyi et al., 2004). Martian sedimentary rocks also frequently exhibit polygonal fracture patterns; some of these are observed in phyllosilicate outcrops (e.g. Loizeau et al., 2007), where they could be desiccation cracks, but the paleoenvironment is uncertain.

And given the evidence for lakes on Titan, including possible dry lakebeds (Stofan et al., 2007), there might be playa-like desiccating environments in some places. This analogy has been proposed for Ontario Lacus, in Titan's southern hemisphere (Lorenz et al., in press). An important component of desiccation polygon formation is a sedimentary material which contracts significantly as it desiccates. I have no idea whether any of the likely sedimentary materials on Titan are analogous to clays on Earth in this sense. Cassini may lack the resolution necessary to confirm polygons, but if the right material exists, giant polygons on Titan might be useful environmental indicators for a future Titan orbiter or balloon.

Polygonal patterns elsewhere are possible, but probably not due to desiccation. Mercury has some very large-scale polygons in the Caloris Basin (Pechmann, 1980), probably due to basin-related tectonics. Could thermal contraction cracks develop on icy satellites? This is unlikely on Titan (near-constant temperature), and cold ice is stronger. Would annual temperature cycles be capable of producing the necessary stresses on other icy satellites?

## References

- Keszthelyi, L., et al., 2004. *Geochem. Geophys. Geosys.* 5, doi: 10.1029/2004GC000758.  
Lachenbruch, A. H., 1962. *GSA Special Paper*, number 70.  
Loizeau, D., et al., 2007. *J. Geophys. Res.* 112, E08S08, doi: 10.1029/2006JE002877.  
Lorenz, R. D., Jackson, B., Hayes, A. *Planet Space. Sci.*, in press.  
McGill, G. E., and Hills, L. S., 1992. *J. Geophys. Res.* 97, 2633-2647.  
Mellon, M. T., Arvidson, R. E., Marlow, J. J., Phillips, R. J., Asphaug, E., 2008. *J. Geophys. Res.* 113, E00A23, doi: 10.1029/2007JE003039.  
Messina, P., Stoffer, P., Smith, W. C., 2005. *Earth-Sci. Reviews* 73, 309-322.  
Neal, J. T., Langer, A. M., Kerr, P. F., 1968. *GSA Bull.* 79, 69-90.  
Pechmann, J. C., 1980. *Icarus* 42, 185-210.  
Pollard, D. D., Aydin, A., 1988. *GSA Bull.* 100, 1181-1204.  
Stofan, E. R., et al., 2007. *Nature* 445, 61-64.  
Tucker, R. M., 1981. *J. Sedim. Petrol.* 51, 779-786.

# Playas and water history in the Southwest since the last ice-age

Christopher Dietl

A Playa is basically defined as the lakebed of a dried lake. A playa can become a permanent lake again through precipitation; However, it will be only ephemeral if the dry conditions persist which led to the lake in the first place. They are of importance for climate research since their sediment sequence can give an insight into the regional climate history and hence data for the evaluation of numerical climate simulations. Fig. 1 shows the Playas in the U.S. (Neal, 1965).

The current knowledge about the water history in the Southwest of the U.S. from the late Pleistocene and Holocene is summarized. Holocene is defined as the period after the last glacial period (12,000 yr B.P.) until the present, Pleistocene as the epoch before the Holocene lasting from 2.588 million yr to 12,000 yr B.P. It is assumed that the reason for the climate changes in such geologically short-term periods ( $10^4$  to  $10^6$  yr) is the development of the insolation caused by orbital changes (Milankovitch Cycles).

The stratigraphy of Willcox Playa, which is also known as Lake Cochise during its wet phase, offers a good opportunity to determine the temporal evolution of precipitation in the Southwest. Researchers took several samples of the lakebed, which indicate, combined with radiocarbon data, that lakes existed in the late glacial period of the ice-age (13,750 -13,400 yr B.P.), the early Holocene (about or before 8900 yr B.P.) and the latter part of the middle Holocene (5000 – 4000 yr B.P.). The first two correlate well with pluvials (extended periods with high precipitation with a timescale of thousand years) suggested by the COHMAP climate model (COHMAP, 1988).

It is assumed, that the pluvial of the late-glacial period, the late-Pleistocene, was caused by a displacement of the Pacific westerlies southwards into the American deserts (COHMAP, 1988). This led to decreased evaporation rates because of lower temperatures and higher winter precipitation (see Fig. 1).

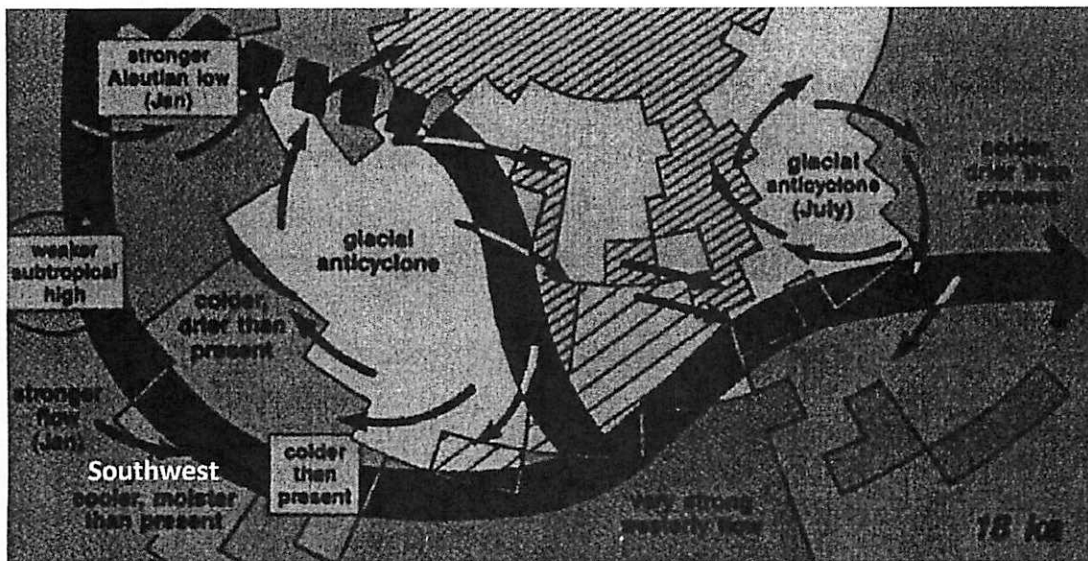


Figure 1 COHMAP climate model showing the splitting of the westerlies 18,000 yr B.P.

The monsoonal circulation was suppressed by these winds, which caused less summer precipitation. However, it is suggested by vegetation fossils (Spaulding and Graumlich, 1986) and the model, that the annual precipitation was almost double the present amount.

After a period of desiccation, water reoccupied the lake in the early Holocene. The COHMAP climate model implies that this pluvial in the Southwest began with the melting of the North American ice sheets. During this period, the modern warmer climate developed. Winter precipitation was reduced, but it was still greater than the present amount. However, the summer precipitation increased, because the summer monsoonal circulation was reestablished. The resulting high annual precipitation led again to a lake.

Lake Cochise desiccated again after this period because of the decrease in summer precipitation at the begin of the Altithermal, a dry period lasting from ca. 7000 to 5000 yr B.P. The last high lake levels are believed to have existed at the end of the Altithermal. Research by Mehringer et al (1967) suggests more humid conditions in this time, which would be consistent with the sediment record.

The time after the middle Holocene is characterized by semiarid conditions, which led to a higher evaporation than precipitation. This represents the current situation, in which only ephemeral lakes can exist.

## References

(Main source) Michael R. Waters, 1988, "Late Quaternary Lacustrine History and Paleoclimatic Significance of Pluvial Lake Cochise, Southeastern Arizona"

COHMAP, 1988, "Climatic Changes of the Last 18,000 Years: Observations and Model Simulations"

James T. Neal, 1965, "Geology, Mineralogy, and Hydrology of U.S. Playas"

Peter J. Mehringer, 1967, "Late quaternary vegetation in the Mohave Desert (U.S.A.)"

W. Geoffrey Spaulding & Lisa J. Graumlich, 1986, "The last pluvial climatic episodes in the deserts of southwestern North America"

Wikipedia: "Ice-age", "Holocene", "Playa", "Pleistocene", "Pluvial", "Altithermal", "Paleoclimatology"  
(all 11/11/09)

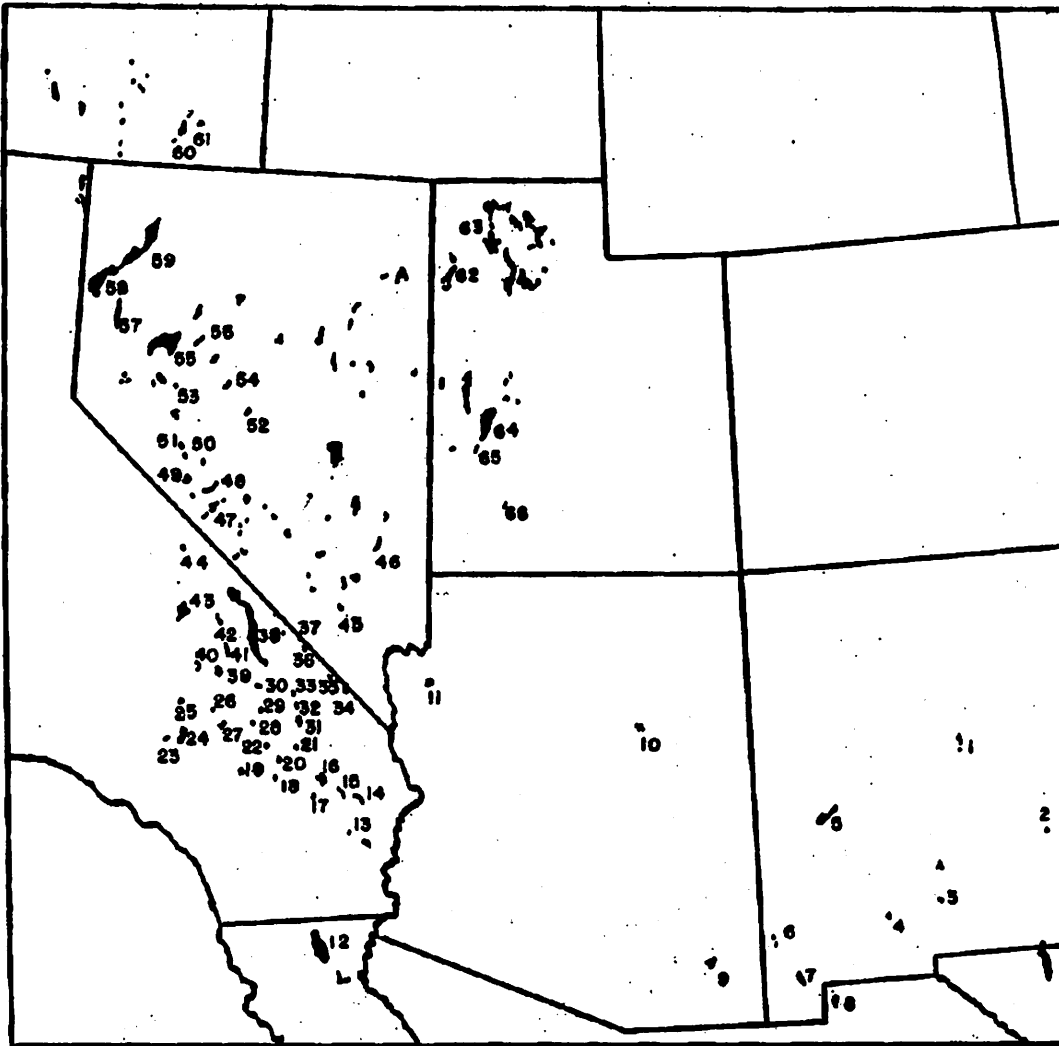


Figure 2 Playas in the U.S. See next page for the according names

Playa Reference List for Figure 2

Geographic names may indicate "lake" or other term; however, all locations here are playas

Map No.	Playa	Map No.	Playa
6	Alkali Flat, Antmas Valley, New Mexico	30	Leach Lake, California
61	Alvord Desert, Oregon	66	Little Salt Lake, Utah
60	Alvord Lake, Oregon	19	Lucerne Lake, California
29	Bicycle Lake, Calif.	2	Marley Playa, New Mexico
48	Big Smoky Valley (Bialr Junction) Playa, Nevada	35	Mesquite Lake, California
52	Big Smoky Valley (Hillett) Playa, Nevada	42	North Panamint Lake, California
59	Black Rock Desert, Nevada	8	Ojos de los Mosquitos, (Hachita Playa) Mexico
82	Bonneville Salt Flats, Utah	43	Owens Lake, California
16	Bristol Lake, Calif.	36	Pahrump Valley Playa, California
21	Broadwell Lake, Calif.	13	Palen Dry Lake, California
15	Caddiz Lake, Calif.	7	Playas Lake, Playas Valley, New Mexico
55	Carson Slak, Nevada	11	Red Lake, Arizona
40	China Lake, Calif.	24	Rogers Lake, California
47	Clayton Valley Playa, Nevada	23	Rosmond Lake, California
49	Columbus Salt Marsh, Nevada	5	San Augustin Plains, New Mexico
28	Coyote Lake, Calif.	39	Searles Lake, California
26	Cuddeback Lake, Calif.	64	Sevier Lake, Utah
17	Dale Lake, Calif.	33	Silurian lake, California
14	Danby Lake, Calif.	32	Silver Lake, California
38	Death Valley Playa, Calif.	54	Smith Creek Valley Playa, Nevada
44	Deep Springs Lake, Calif.	58	Smoke Creek Desert, Nevada
46	Delmar Dry Lake, Nev.	31	Soda Lake, California
63	Great Salt Lake Playa Complex, Utah	51	Soda Spring Valley (Tunning) Playa, Nevada
27	Harper Lake, Calif.	50	Soda Spring Valley (Mina) Playa, Nevada
56	Humboldt Salt Marsh, Nev.	18	Sogey Lake, California
45	Indian Springs Playa, Nev.	41	South Panamint Lake, California
34	Ivampah Lake, Calif.	37	Stewart Valley Playa, Nevada
25	Koehn Lake, Calif.	22	Troy Lake, California
53	Labou Flat, Nevada	4	Uvas Playa, New Mexico
1	Laguna del Perro (Estanola Playa), New Mexico	65	Wah Wah Valley Hardpan, Utah
12	Laguna Salada, Mexico	9	Wallcox Dry Lake, Arizona
3	Lake Lucero, New Mexico	57	Winnemucca Lake, Nevada
20	Lavie Lake, Calif.	10	Winslow Playas, Arizona

# Evaporites

---

- A (primary) evaporite is a mineral that was precipitated from a saturated solution where the water was removed by solar-driven evaporation
- Evaporite formation, deposition, and preservation depends on 3 things:
  - A surface or near-surface body of water that is saline enough for salts to precipitate out of solution and be preserved.
  - There must be space in a sedimentary depression to accommodate the salts.
  - The burial environment must not allow significant flow-through of undersaturated fluids which would dissolve and remove the salts.
- Evaporites accumulate in arid regions when more water is leaving via evaporation than is entering via rainfall, snowmelt, surface, or subsurface inflow.
  - Tectonic basins
  - Interdune depressions
  - Wind-deflation hollows
  - Abandoned fluvial valleys
  - Craters of any type
  - Interior drainage depressions
- Salt sources:
  - Marine water
  - Salts deposited by rainwater/atmospherically produced salts (perchlorate)
  - Leaching from rocks upstream
- Evaporite deposition is inversely related to solubility with the least soluble minerals precipitating out first

Mineral Name	Chemical Formula	solubility @ 25°C (mol/L)
dolomite	$\text{CaMg}(\text{CO}_3)_2$	2.99E-04
calcite	$\text{CaCO}_3$	5.21E-04
celestite	$\text{SrSO}_4$	6.25E-04
magnesite	$\text{MgCO}_3$	8.41E-04
gypsum	$\text{CaSO}_4 \cdot 2\text{H}_2\text{O}$	1.52E-02
anhydrite	$\text{CaSO}_4$	2.28E-02
glauberite	$\text{Na}_2\text{Ca}(\text{SO}_4)_2$	0.426
sylvite	KCl	4.797
halite	NaCl	6.1
kieserite	$\text{MgSO}_4 \cdot \text{H}_2\text{O}$	6.251

- Formation of evaporites in a playa
  - Salt pans usually form in the lowest parts of the playa surface (makes sense, this is where the water will stay the longest) surrounded by extensive mudflats.
  - Pan areas can be small features or very large (9000 km<sup>2</sup> pan in Salar di Uyuni, Bolivia)
  - Salt crusts dominated by halite, but other minerals such as gypsum, mirabilite, and trona can be important.
  - Final buried sediment is a thick bedded-salt composed of randomly aligned recrystallized evaporites

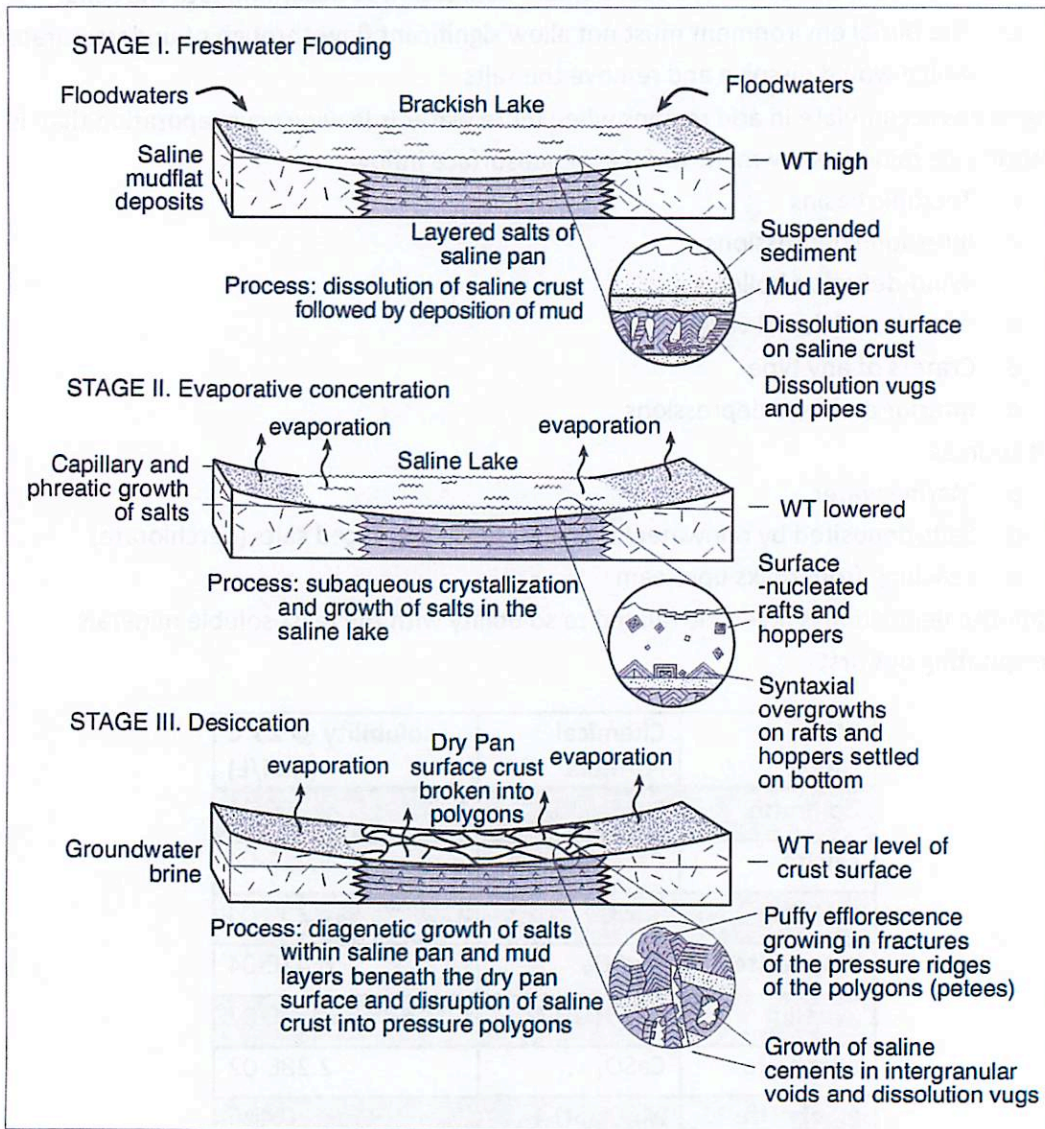
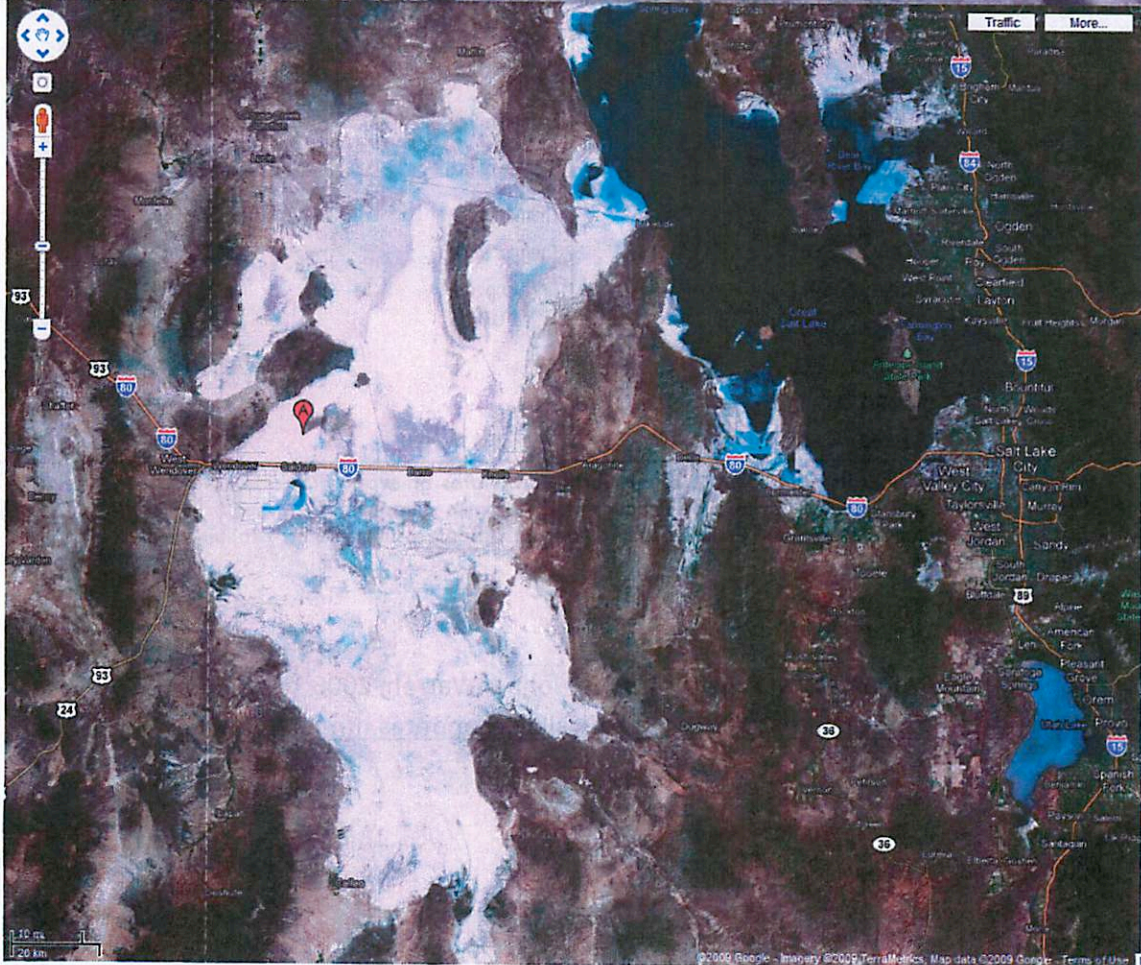
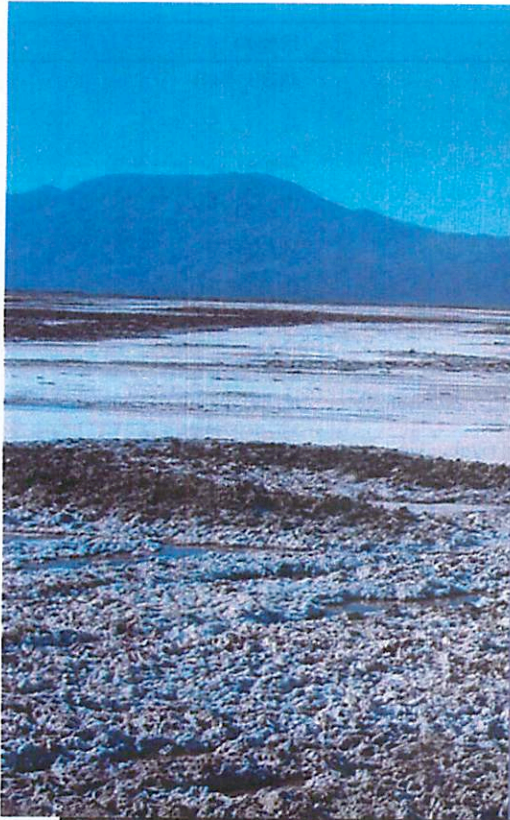


Figure 3.30. Evolution of a depositional cycle in a saline pan setting (after Lowenstein and Hardie, 1985).

- Planetary Connection
  - Evaporites detected in Nakhilites
  - Evaporites (sulfates) seen from orbit by OMEGA and CRISM, by the Mars Exploration Rovers, and Phoenix.





Mineral	Formula	Mineral	Formula
Anhydrite	CaSO <sub>4</sub>	Leonhardtite	MgSO <sub>4</sub> ·4H <sub>2</sub> O
Antarctite	CaCl <sub>2</sub> ·6H <sub>2</sub> O	Leonite	MgSO <sub>4</sub> ·K <sub>2</sub> SO <sub>4</sub> ·4H <sub>2</sub> O
Aphthitalite (glaserite)	K <sub>2</sub> SO <sub>4</sub> ·(Na,K)SO <sub>4</sub>	Loewite	2MgSO <sub>4</sub> ·2Na <sub>2</sub> SO <sub>4</sub> ·5H <sub>2</sub> O
Aragonite **	CaCO <sub>3</sub>	Mg-calcite **	(Mg,Ca <sub>1-x</sub> )CO <sub>3</sub>
Bassanite	CaSO <sub>4</sub> ·1/2H <sub>2</sub> O	Magnesite**	MgCO <sub>3</sub>
Bischofite	MgCl <sub>2</sub> ·6H <sub>2</sub> O	Meyerhoffite	Ca <sub>2</sub> B <sub>5</sub> O <sub>11</sub> ·7H <sub>2</sub> O
Bloedite (astrakanite)	Na <sub>2</sub> SO <sub>4</sub> ·MgSO <sub>4</sub> ·4H <sub>2</sub> O	Mirabilite	Na <sub>2</sub> SO <sub>4</sub> ·10H <sub>2</sub> O
Borax (tincal)	Na <sub>2</sub> B <sub>4</sub> O <sub>7</sub> ·10H <sub>2</sub> O	Nahcolite	NaHCO <sub>3</sub>
Boracite	Mg <sub>3</sub> B <sub>7</sub> O <sub>13</sub> Cl	Natron	Na <sub>2</sub> CO <sub>3</sub> ·10H <sub>2</sub> O
Burkeite	Na <sub>2</sub> CO <sub>3</sub> ·2Na <sub>2</sub> SO <sub>4</sub>	Nitratite (soda nitre)	NaNO <sub>3</sub>
Calcite**	CaCO <sub>3</sub>	Nitre (salt petre)	KNO <sub>3</sub>
Carnallite	MgCl <sub>2</sub> ·KCl·6H <sub>2</sub> O	Pentahydrate	MgSO <sub>4</sub> ·5H <sub>2</sub> O
Colemanite	Ca <sub>2</sub> B <sub>5</sub> O <sub>11</sub> ·5H <sub>2</sub> O	Pirssonite	CaCO <sub>3</sub> ·Na <sub>2</sub> CO <sub>3</sub> ·2H <sub>2</sub> O
Darapskite	NaSO <sub>4</sub> ·NaNO <sub>3</sub> ·H <sub>2</sub> O	Polyhalite	2CaSO <sub>4</sub> ·MgSO <sub>4</sub> ·K <sub>2</sub> SO <sub>4</sub> ·H <sub>2</sub> O
Dolomite**	Ca <sub>(1-x)</sub> Mg <sub>(1-x)</sub> (CO <sub>3</sub> ) <sub>2</sub>	Proberite	NaCaB <sub>5</sub> O <sub>9</sub> ·5H <sub>2</sub> O
Epsomite	MgSO <sub>4</sub> ·7H <sub>2</sub> O	Priceite (pandermite)	CaB <sub>4</sub> O <sub>10</sub> ·7H <sub>2</sub> O
Ferronatrinite	3NaSO <sub>4</sub> ·Fe <sub>2</sub> (SO <sub>4</sub> ) <sub>3</sub> ·6H <sub>2</sub> O	Rinneite	FeCl <sub>2</sub> ·NaCl·3KCl
Gaylussite	CaCO <sub>3</sub> ·Na <sub>2</sub> CO <sub>3</sub> ·5H <sub>2</sub> O	Sanderite	MgSO <sub>4</sub> ·2H <sub>2</sub> O
Glauberite	CaSO <sub>4</sub> ·Na <sub>2</sub> SO <sub>4</sub>	Schoenite (picromerite)	MgSO <sub>4</sub> ·K <sub>2</sub> SO <sub>4</sub> ·6H <sub>2</sub> O
Gypsum	CaSO <sub>4</sub> ·2H <sub>2</sub> O	Shortite	2CaCO <sub>3</sub> ·Na <sub>2</sub> CO <sub>3</sub>
Halite	NaCl	Sylvite	KCl
Hanksite	9Na <sub>2</sub> SO <sub>4</sub> ·2Na <sub>2</sub> CO <sub>3</sub> ·KCl	Syngenite	CaSO <sub>4</sub> ·K <sub>2</sub> SO <sub>4</sub> ·H <sub>2</sub> O
Hexahydrate	MgSO <sub>4</sub> ·6H <sub>2</sub> O	Tachyhydrite	CaCl <sub>2</sub> ·2MgCl <sub>2</sub> ·12H <sub>2</sub> O
Howlite	H <sub>3</sub> Ca <sub>2</sub> SiB <sub>3</sub> O <sub>14</sub>	Thernadite	Na <sub>2</sub> SO <sub>4</sub>
Ikaite**	CaCO <sub>3</sub> ·6H <sub>2</sub> O	Thermonatrinite	NaCO <sub>3</sub> ·H <sub>2</sub> O
Inyoite	Ca <sub>2</sub> B <sub>6</sub> O <sub>11</sub> ·13H <sub>2</sub> O	Tincalconite	Na <sub>2</sub> B <sub>4</sub> O <sub>7</sub> ·5H <sub>2</sub> O
Kainite	4MgSO <sub>4</sub> ·4KCl·11H <sub>2</sub> O	Trona	NaHCO <sub>3</sub> ·Na <sub>2</sub> CO <sub>3</sub>
Kernite	Na <sub>2</sub> B <sub>4</sub> O <sub>7</sub> ·4H <sub>2</sub> O	Tychite	2MgCO <sub>3</sub> ·2NaCO <sub>3</sub> ·Na <sub>2</sub> SO <sub>4</sub>
Kieserite	MgSO <sub>4</sub> ·H <sub>2</sub> O	Ulexite	NaCaB <sub>5</sub> O <sub>9</sub> ·5H <sub>2</sub> O
Langbeinite	2MgSO <sub>4</sub> ·K <sub>2</sub> SO <sub>4</sub>	Van'thoffite	MgSO <sub>4</sub> ·3Na <sub>2</sub> SO <sub>4</sub>

Table 1.1. Major evaporite minerals: less saline alkaline earth carbonates or evaporitic carbonates are indicated by \*\*, the remainder are the more saline evaporite salts. Documented dolomite composition ranges from Ca<sub>1.16</sub>Mg<sub>0.84</sub>(CO<sub>3</sub>)<sub>2</sub> to Ca<sub>0.96</sub>Mg<sub>1.04</sub>(CO<sub>3</sub>)<sub>2</sub>. Less common evaporite minerals, such as borates, iodates, nitrates and zeolites are not listed here, but are discussed in detail in Chapter 11.

#### References:

*Evaporites: Sediments, Resources, and Hydrocarbons*. John K Warren, 2006  
<http://dynamic-earth.blogspot.com/2008/04/death-valley-evaporites.html>

# Clay Dunes

Ingrid *better-than-my-better-half* Daubar

## CLAY

Note on terminology: "Clay" → grain size (right)

"Clay" **composition**: hydrous phyllosilicates that form most of that particle size range.

- Include kaolinites, serpentinites, illites, micas, chlorites, smectites, montmorillonites, etc.
- Require H<sub>2</sub>O to form.
- Types & assemblages are determined by amount, salinity, pH of water involved, as well as parent material.

## CLAY DUNES

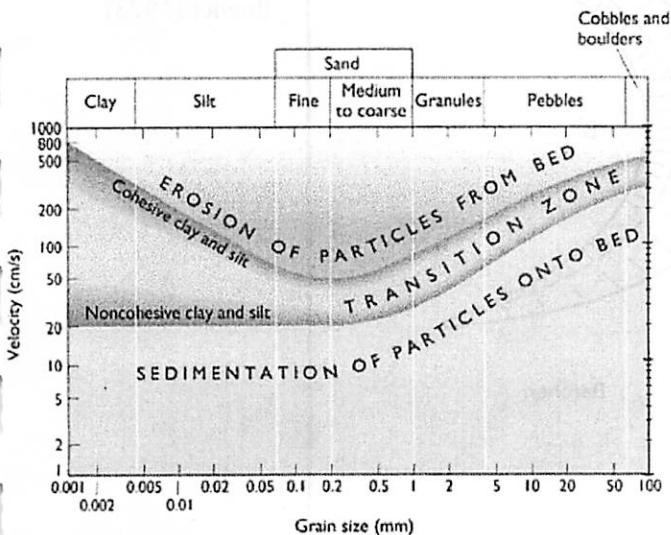
Dunes are usually made of **quartz** - abundant, thermodynamically stable, very resistant to mechanical & chemical weathering.

Clays (and silts) are rare in dunes because they're easily suspended, carried far from source, & deposited in thin mantles instead of dunes.

20 wt% clay content enough to cause morphological differences  
== clay dune or "lunette"

Wentworth (1922)	U.S. Bureau of Soils	diameter (millimetres)
boulders		20-48
		1024
cobble		512
		256
pebbles		128
		64
		32
		16
granules		8
		4
sand	gravel	2
		1
		1/2
		1/4
		1/8
silt	silt	1/16
		0.05
		1/32
		1/64
		1/128
clay	clay	1/256
		1/512
		1/1024
		1/2048

Wentworth scale of grain sizes.  
<http://www.glaucus.org.uk/Wentworth.htm>



Hjulstrom plot for grain transport under water. For wind transport (lower-density medium), higher velocities are required to move same size particle.  
<http://tinyurl.com/y8k5kyl>

Clay dunes form:

- At the edges of salt flats (playas)
  - Salts required: inhibit vegetation that would trap sediment on playa floor, and for efflorescence process (below) to form aggregates.
  - Water required: concentrates & distributes salts, stabilizes dunes.
- Require strong, mostly unidirectional winds in the hot dry season
- High, rapid evaporation rates

**Formation Process:**

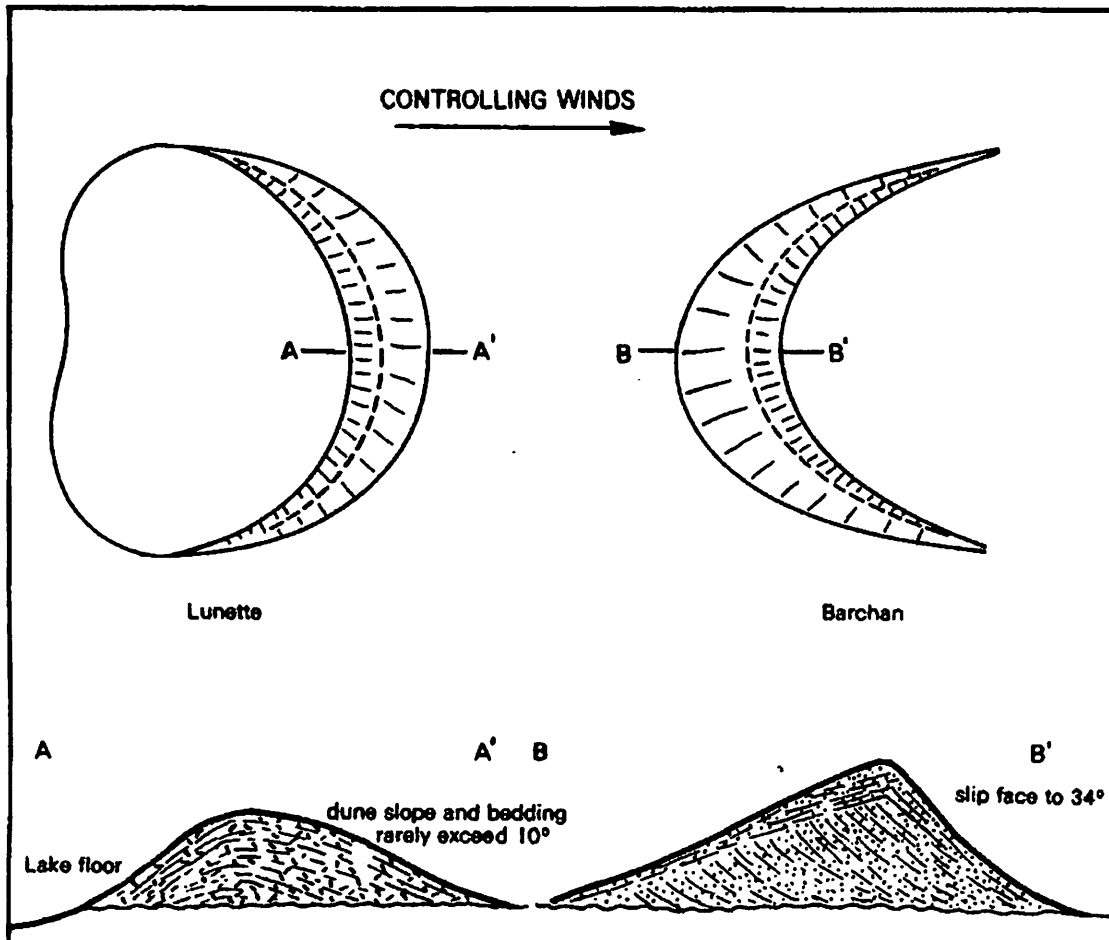
- Evaporite salts in upper layer of mud crust *effloresce* (dry, turn into a fine powder) or thin edges of mud cracks curl up & fall apart
  - → Sand-sized aggregates of clay minerals
- Pellets deposited at edge during dry season.
- Clays ab/adsorb water from air & stabilize
  - Most of the clay stays dry, but upper layer gets wet & regains plasticity
- Deposition during mid-late part of dry season → indicator of past seasonal conditions.

**Resulting morphology:**

- Transverse ridges following salt-flat edge/dominant wind direction
- Aerial extent ~ source region.
- Height ~5-15 meters (don't get very high)

**Differences compared to typical quartz dunes:**

- Often crescent-shaped, but horns point *toward* wind instead of away
- Low-angle layering (dip < ~ 10°) – if visible – bedding only forms if deposition is rapid; slow deposition results in diffuse banding.
- Parallel bedding
- Slopes usually < 15°, steeper side to windward
- No steep slip faces → no avalanches or truncated cross-bedding
- Stabilize rapidly so don't migrate



Planform (top) and cross-section (bottom) of clay dunes (L) compared to barchan sand dunes (R). Bowler (1973)

## WILLCOX PLAYA CLAY DUNES

- 32 °C mean annual temp
- 469 mm mean annual precipitation
- 1550 mm mean annual evaporation from a theoretical lake surface

In Willcox Playa mud (& thus presumably in dunes) these clay minerals dominate:  
illite, minor montmorillonite, vermiculite, trace kaolinite & chlorite

**Remote Sensing:** (See color aerial photos)

*Particle size:*

Morphology + wind direction

Thermal inertia - but non-unique, average over one skin depth

Affected by: induration; porosity (aggregates); airfall dust cover

*Composition:*

Spectroscopy

## PLANETARY CONNECTION:

*Clay dunes → presence of water near the surface*

*Seasonal, repeated cycle*

**Mars?**

- Clay dunes not seen in cold terrestrial deserts (yet?).
- Phyllosilicates detected from orbit - in ancient Noachian bedrock, not dunes.
- Aggregates of dust (clay-sized) seen by rovers, but not phyllosilicate composition.
- Transverse Aeolian Ridges?

**Titan**

- Titanian dune compositions more likely organics and/or ices.

## SELECTED REFERENCES

Bagnold, R.A. (1954) *The physics of blown sand and desert dunes*. London, Methuen.

Balme, M. (2008) Transverse Aeolian Ridges (TARs) on Mars. *Geomorphology*, Volume 101, Issue 4, Pages 703-720.

Bowler, J. M. (1973) Clay Dunes: Their occurrence, formation and environmental significance. *Earth Science Reviews*, Volume 9, Issue 4, p. 315-338.

Coffey, G.N. (1909) Clay Dunes. *The Journal of Geology*, Vol. 17, No. 8, pp. 754-755 .

Huffman, G.G. and W.A. Price (1949) Clay dune formation near Corpus Christi, Texas. *Journal of Sedimentary Research*; 19: 118 - 127.

Lorenz, R. D., et al. (2008), Titan's inventory of organic surface materials, *Geophys. Res. Lett.*, 35, L02206.

Martin, P.S. (1963) Geochronology of Pluvial Lake Cochise, Southern Arizona. II. Pollen Analysis of A 42-Meter Core. *Ecology*, Vol. 44, No. 3, pp. 436-444.

Murchie, S. L., et al. (2009), A synthesis of Martian aqueous mineralogy after 1 Mars year of observations from the Mars Reconnaissance Orbiter, *J. Geophys. Res.*, 114, E00D06.

Poulet, F., et al. (2005), Phyllosilicates on Mars and implications for early Martian climate, *Nature*, 438, 623-627.

Schreiber, J.F. et al. (1972) Sedimentologic Studies in the Willcox Playa area, Cochise County, Arizona, in *Playa Lake Symposium*, pub. International Center for Arid and Semi-Arid Land Studies, Texas Tech, pp 133 - 184.

Sullivan, R., et al. (2008), Wind-driven particle mobility on Mars: Insights from Mars Exploration Rover observations at "El Dorado" and surroundings at Gusev Crater, *J. Geophys. Res.*, 113, E06S07, doi:10.1029/2008JE003101.

# HOODOOS

Jamie Molaro

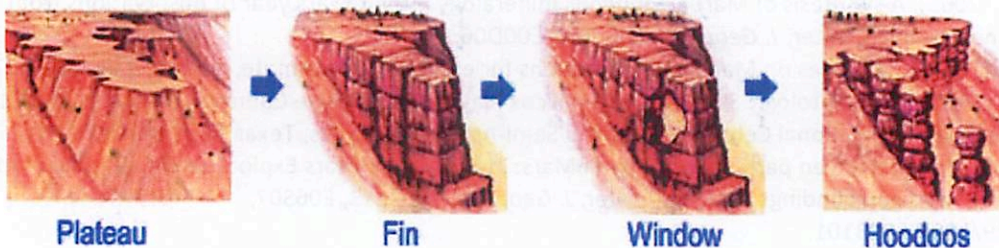
## Formation of Hoodoos

In arid, sandy, clayey environments there is not enough moisture, and too much time, between cloudbursts for any significant amount of vegetation to grow. As a result, water that does come through easily washes gullies and valleys into the landscape. This type of landscape is referred to as badlands. Erosion in badlands, or indeed any environment, does not take place at the same rate in all localities. Particular landscape features may cause more or less ablation and dissolution than others, so that "islands" are formed around which erosion takes place at a faster rate. Water washes off the tops and collects in deeper places adjacent to or below the islands. Eventually, a series of these islands will stand out in an area, the rest of which has been eroded away. These features typically are pyramidal shaped, and depending on the region's geology may become mesas, plateaus, or buttes, accompanied by valleys, gullies, and ravines. The figure below is of the The Chinle Badlands at Grand Staircase-Escalante National Monument.

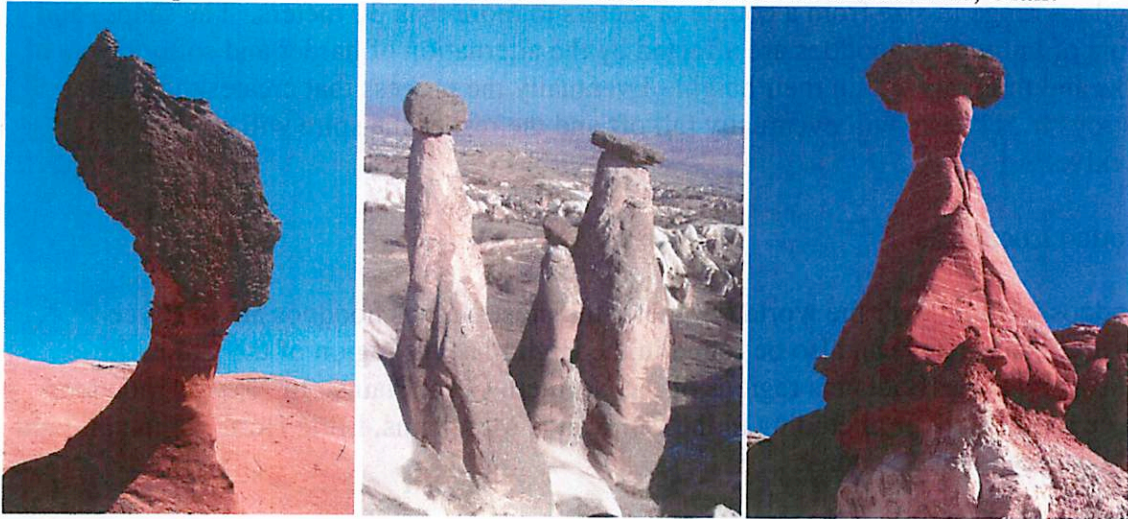


A slightly more extreme version of this processes produces structures that instead of being pyramidal, have a mushroom shaped form. These are what we call hoodoos (also tent rocks, fairy chimneys, earth pyramids). Images of hoodoos are on the next page. The formation of these structures is similar to that of the mesas, but in the process of erosion by water we see what is called the "tea pot effect." The teapot effect

is simply that which is encountered when water poured out of a teapot runs down the spout instead of straight out into the cup. Hoodoos typically form in areas where there is a thick layer of tuff (volcanic ash) covered by a thin layer of basalt, or other volcanic rock, that is more resistance to water erosion. Water runs around the "brim" of the "hat" and down the "neck," instead of straight off the top and down the sides like in a regular pyramidal process. Frost wedging can also contribute to the process, as water freezes in small cracks, expands, and widens the crack causing additional deformation to the rock and thereby aiding in the water erosion process.



These figures show The Queen's Head in Taiwan, hoodoos in Cappadocia, Turkey, and a toadstool-shaped hoodoo at Grand Staircase-Escalante National Monument, Utah.



### The Teapot Effect

The teapot effect can be explained through the interplay of hydrodynamical forces as a sheet flow moves from shear (along the surface) to extensional (falling) flow. A number of different variables affect this process, including speed of the flow, viscosity of the liquid, and geometry and wettability of the lip. Hysteresis arises due to parameters like contact angle and surface roughness. The process is complex and if you wish to see a full theoretical and numerical study on the subject please see the references. See Figure on next page.

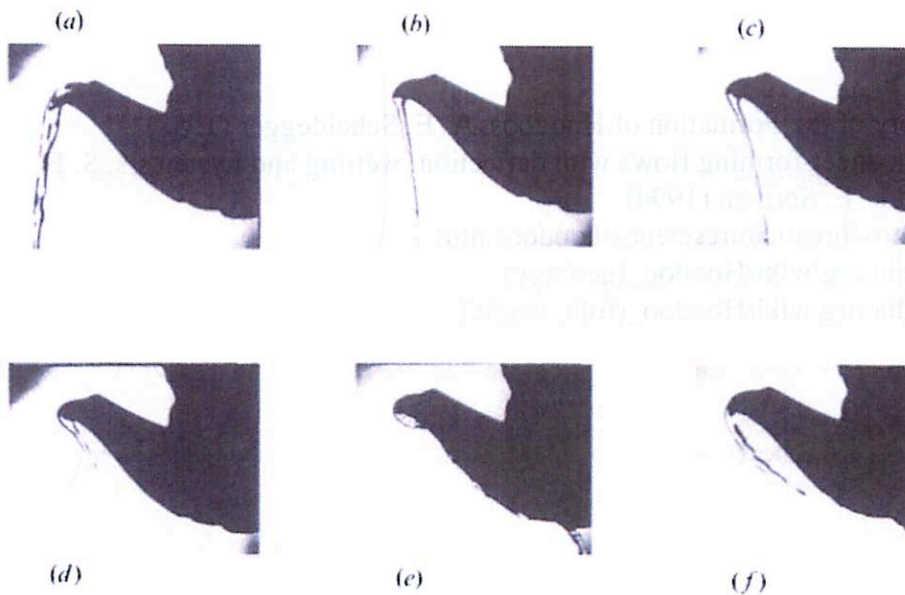


FIGURE 2. Photographs of a water stream flowing from the spout of a teapot. The flow rate is decreased from (a) to (e), and increased from (e) to (f).

## **Hoodoo Characteristics**

Hoodoos range in size from a couple of meters to more than 30 meters. The shapes and colors of individual hoodoos are affected by the alternation of harder and softer layers of rocks and minerals within their height. Eventually the process that creates the hoodoo destroys it. The cap will eventually fall off and the rest of the spire will erode away quickly.

## **Hoodoo Locations**

Hoodoos form all over the world. Some of the most famous hoodoos are in Bryce Canyon, Utah. They can also be found in the High Plateaus region of the Colorado Plateau and in the Badlands regions of the Northern Great Plains. In Arizona, hoodoos can be found all over, including in the Chiricahua Mountains, Little Horn Mountains, and in the valley around Sedona.

## **Fun Facts**

Hoodoo is a form of folk magic practiced predominantly by African-Americans. It is a tradition of magical practice that developed from many separate religions, cultures, and practices, including many from African, Native American, and European traditions. Oddly, while hoodoo is a sort of trans-cultural phenomena, the dominant world view of hoodoo is strongly Christian, and God himself is seen as the archetypal hoodoo doctor. Many other Biblical figures are recast as hoodoo doctors as well, such as Moses. The Bible itself is considered "the great conjure book" and is used (particularly the Psalms) as a source of spells. Regional synonyms for hoodoo include *conjunction*, *conjure*, *witchcraft*, or *rootwork*.<sup>[4]</sup>

## **References:**

A Physical Theory of the Formation of Hoodoos, A. E. Scheidegger (1958)

The teapot effect: sheet-forming flows with deflection, wetting and hysteresis, S. F. Kistler and L. E. Scriven (1994)

<http://www.nps.gov/brca/naturescience/hoodoos.htm>

[http://en.wikipedia.org/wiki/Hoodoo\\_\(geology\)](http://en.wikipedia.org/wiki/Hoodoo_(geology))

[http://en.wikipedia.org/wiki/Hoodoo\\_\(folk\\_magic\)](http://en.wikipedia.org/wiki/Hoodoo_(folk_magic))





# An Intro to the Turkey Creek Eruption

by Tom 'Catfish' Schad

'High-angle extensional faulting and erosion have combined in the Chiricahua Mountains to expose a three-dimensional view of the volcanic and hypabyssal levels of a mid-Tertiary ash flow caldera'

-du Bray & Pallister (1991)

## THE SURFACE LAYER OF THE CALDERA REGION

See figure on next page

'Basement' Precambrian crystalline rock interrupted by complex sequence of **volcanism** and tectonic deformation



Turkey Creek Caldera - 20 km diameter collapse structure  
1000 times larger than Mount St. Helen's 1980 eruption

High-silica rhyolite and dacite primarily cover the caldera region. Argon dating of rhyolite Canyon tuff and prophyry dacite suggests formation of caldera at ~26.9 Ma (i.e. transitional period between mid-Tertiary compression and Basin and Range extension). This is the youngest volcanic region recognized near the Chiricahua Mountains.

Thick dacite and rhyolites lavas and domes formed at ~28 Ma are exposed near Cave Creek, Cochise Head, and Pinery Canyon.

To the southeast, moat rhyolite lava and rhyolite canyon tuff have formed in an older caldera, the Portal Caldera.

Evidence for extension during formation

- Rhyolite Canyon Tuff outflowed north and accumulated in paleobasin at Chiricahua Nat'l Monument. Flows also to the south.
- Cogenic Rhyolite Canyon Tuff and dacite prophyry are offset and covered by younger rhyolite lavas in NW.

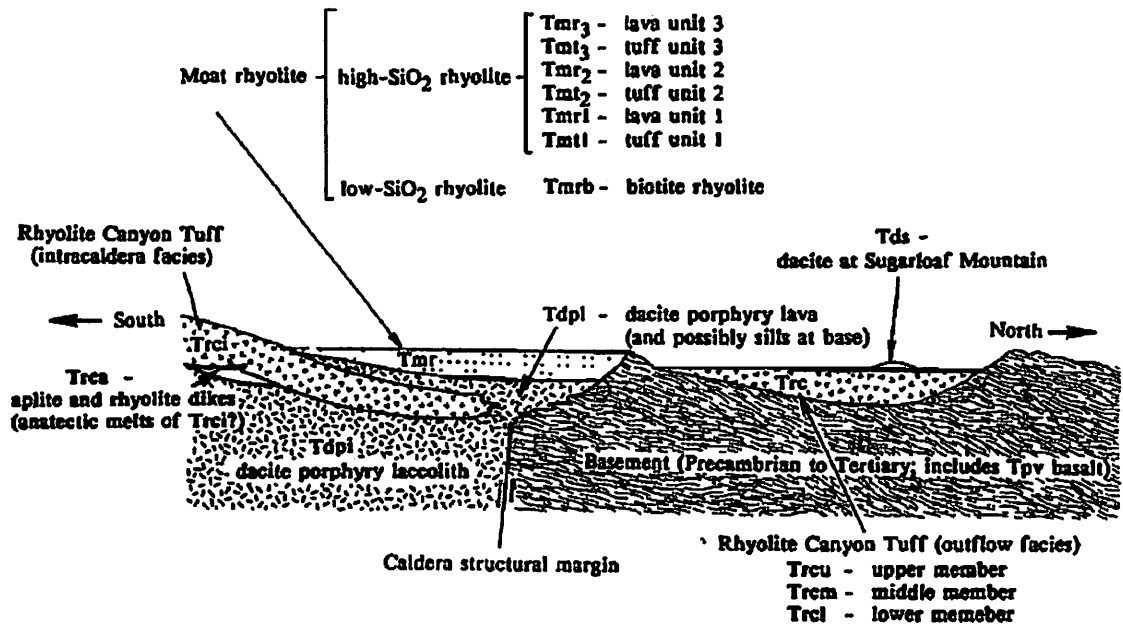


Fig. 2. Schematic cross section of the northern margin of the Turkey Creek caldera, showing stratigraphic and structural relations of principal rock units, and rock unit symbols (acronyms) used in text; not to scale.

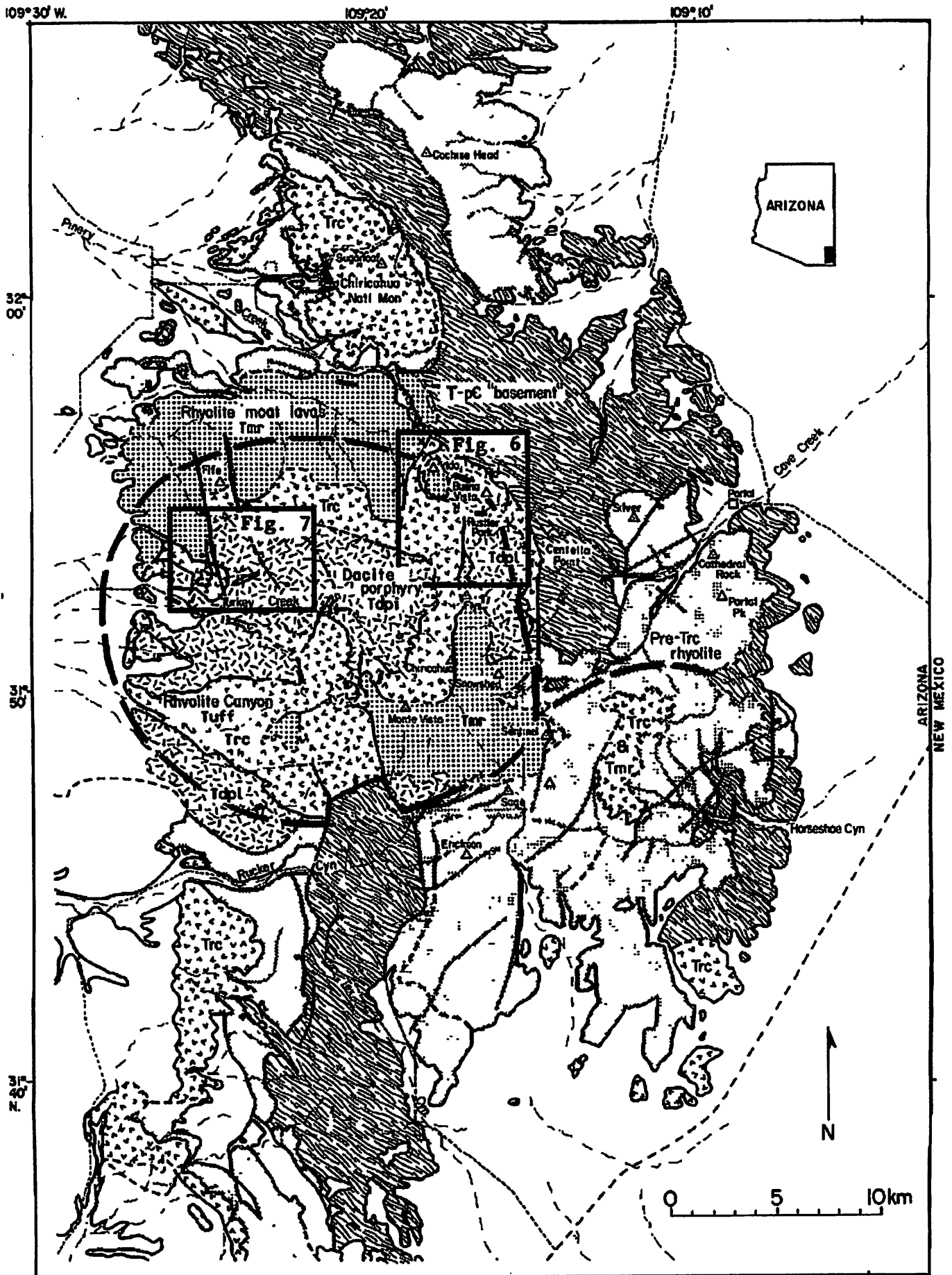


Fig. 1. Geologic index map of the Chiricahua Mountains [after Marjaniemi, 1969]. Trc, Rhyolite Canyon Tuff; Tmr, moat rhyolite; Tdpi, dacite porphyry resurgent intrusion; Tdpl, dacite porphyry lava; T-pC, Tertiary to Precambrian basement rocks. Dense stipple pattern indicates precaldera Tertiary volcanic rocks, mostly rhyolite. Approximate structural boundary of the Turkey Creek caldera and NW boundary of the Portal caldera are indicated by heavy lines.

# PROPOSED EVOLUTIONARY STAGES OF THE TURKEY CREEK CALDERA

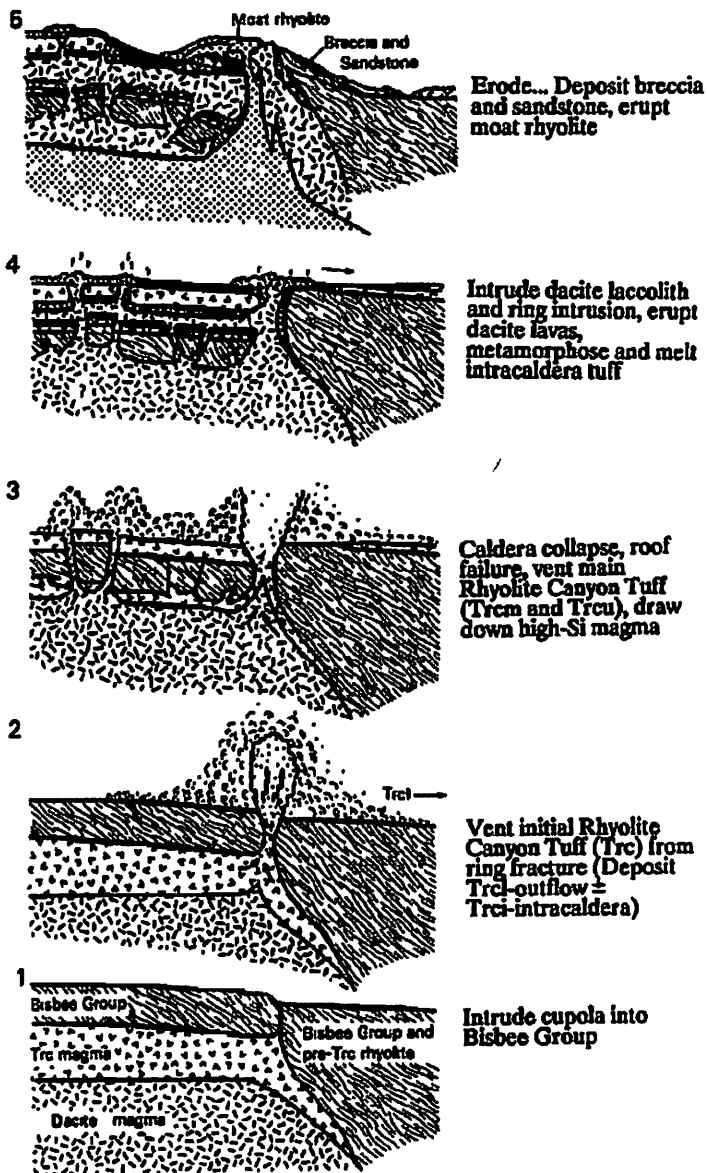


Fig. 18. Proposed structural model for stages in the evolution of the Turkey Creek caldera. Unit identifiers as in Figure 2.

## Stage 5

- Erosion and clastic deposition
- Four cycles of high-silica rhyolite lava fills moat.

## Stage 4

- Dacite porphyry eruption from ring vents and accumulation in caldera moat
- Laccolith formation by dacite intrusion within intracaldera tuff.
- Roof breccia/melt forms as interface

## Stage 3: ~26.9 Ma

- Collapse of Turkey Creek caldera
- Eruption of Rhyolite Canyon Tuff (lower tuff material not deposited in caldera)
- Rise and eruption of dacite porphyry from ring vents, thick dacite lavas in caldera moat.

## Stage 2: ~ 28 Ma

- Shallow crustal compositional stratified magma chamber develops
- Eruption of a thick series of dacite and rhyolites lavas and domes
- collapse of adjacent Portal caldera

## Stage 1: ~32-28 Ma

- Minor alkali basalt volcanism
- Dacite and rhyolite lavas
- Pyroclastic flows (i.e. Faraway Ranch Formation)
- emplacement of small granodiorite to granite plutons

## RESOURCES

1. Du Bray, E.A. & Pallister, J.S. (1991) JGR, 96, B8, 13435
2. Chronic, H., 1986 'Pages of Stone: The Mountaineers, v.3, p 79-85
3. Jackson, E., 1970, The Natural History of Chiricahua National Monument, Arizona: Globe, AZ, Southwest Parks and Monuments Assoc. (out of print)
4. Morrison, R.B., 1991, 'Quaternary geology of the southern Basin and Range province, in Morrison, R.B., ed. Quaternary nonglacial geology, v. K-2, p. 353-371

# "How the West was Widened"<sup>1</sup>: Plate Tectonics and Basin and Range Formation

Catherine Elder

## 1 Introduction

The Basin and Range province in the Southwestern portion of North America is characterized by normal faulting, high heat flow, thin crust, and a high regional elevation. These features are typical of extensional areas throughout the world (Zoback *et al.* 1981). In the case of the Basin and Range region, the extension was probably caused by plate interactions along the western plate boundary of North America changing the stress pattern in the western portion of North America. Currently, the Basin and Range region consists of regionally parallel ranges separated by basins filled with Tertiary-Quaternary sediments (Zoback *et al.* 1981). Estimates for the total amount of extension vary significantly. The study of planar faults in a single basin predict 5-15% extension (Zoback *et al.* 1981, Thompson and Burke 1974). Gravity constraints on vertical offsets and magnetic constraints on lateral offsets of dikes predicts 17-23% extension (Zoback *et al.* 1981). Variation in crustal thickness predicts crustal extension of 35 - 100% in the western and eastern parts of the Northern Basin and Range region and 10-15% extension in the central part (Proffett 1977). Some of the discrepancy between these estimates may be due to multiple periods of extension (Zoback *et al.* 1981).

## 2 Geologic Setting

The Basin and Range region is located near to boundaries with the Pacific plate, the Cocos plate and the Juan de Fuca plate. The Laramide orogeny which built the Rocky Mountains and affected the geology of western North America started while the Kula plate was being subducted under the North American plate (English *et al.* (2003), Fig. 1). Compression during the Laramide orogeny resulted in large basement uplifts bounded by thrust faults (Zoback *et al.* 1981). The Kula plate eventually went completely under the North American plate, and subduction of the Farallon plate began. The orogenesis began to move eastward in North America probably due to flat slab subduction (English *et al.* 2003). Compressional tectonism ended between 40 and 50 Ma possibly because of a worldwide reorganization of plate motions implied by the 40 Ma bend in the Hawaiian-Eperor seamount chain (Zoback *et al.* 1981). When the Farallon-Pacific ridge collided with the trench sometime between 20 and 30 Ma, the San Andreas transform fault began to develop, because the motion of the Pacific plate was parallel to the western edge of North America (Zoback *et al.* 1981, Sonder and Jones 1999). The volcanic arc that had developed by about 20 Ma shortened as the San Andreas transform lengthened (Fig. 2) and extension began behind the arc (Zoback *et al.* 1981).

---

<sup>1</sup>Title from Sonder and Jones (1999)

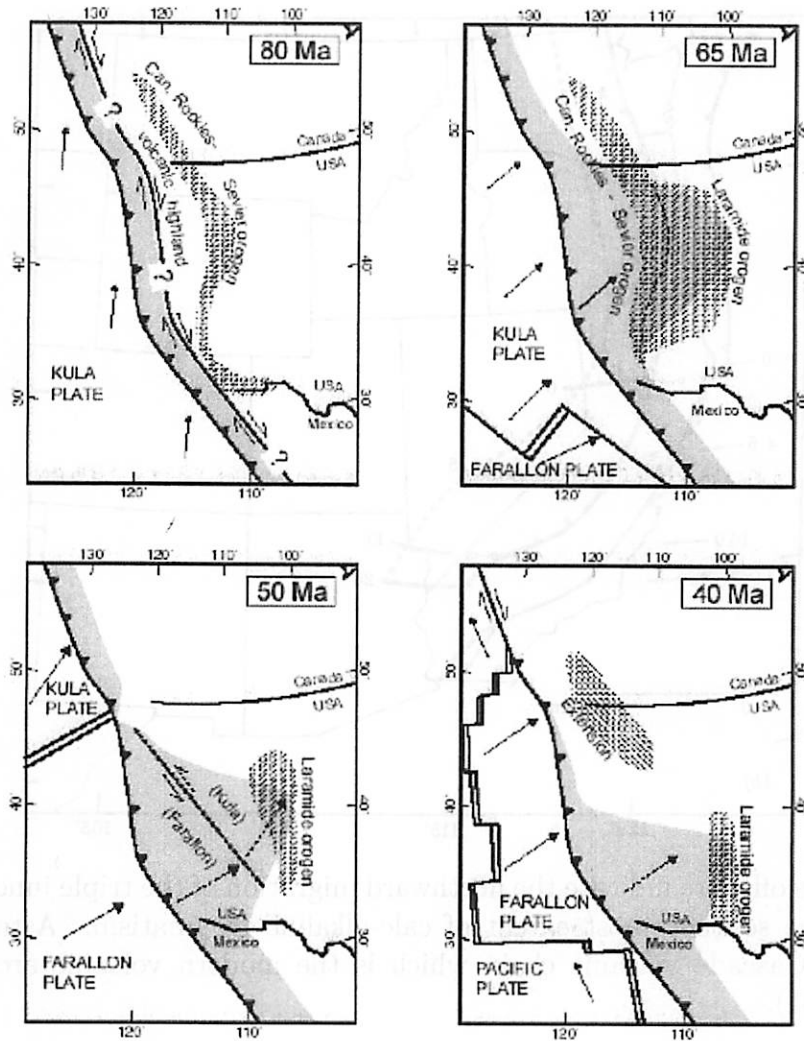


Figure 1: The evolution of the Laramide orogeny starting with Kula oblique subduction 80 Ma and followed by horizontal subduction of the Kula plate 65 Ma, transition between the Kula and Farallon plates 50 Ma, horizontal subduction of the Farallon plate 40 Ma. The shaded area represents the forearc contact between North America and subducting slabs. The diagonal area represents regions of orogeny or extension (figure from a lecture slide in the “Orogenic Systems class I took”).

### 3 Pre-Basin and Range Extension

Extension in western North America began as early as 30 Ma. The first ~20 Myr of extension differed in structural style and associated magmatism than the last 6 Myr of basin-range extension which forms the currently observed morphology (Zoback *et al.* 1981). The extension was produced by shallow brittle deformation on closely spaced normal faults which kept local topographic relief low (Zoback *et al.* 1981). Evidence for early extension in the Basin and Range region is seen in strata exposed in uplifted blocks that are tilted on slip faults that predate uplift of the range. The older faults are truncated by younger

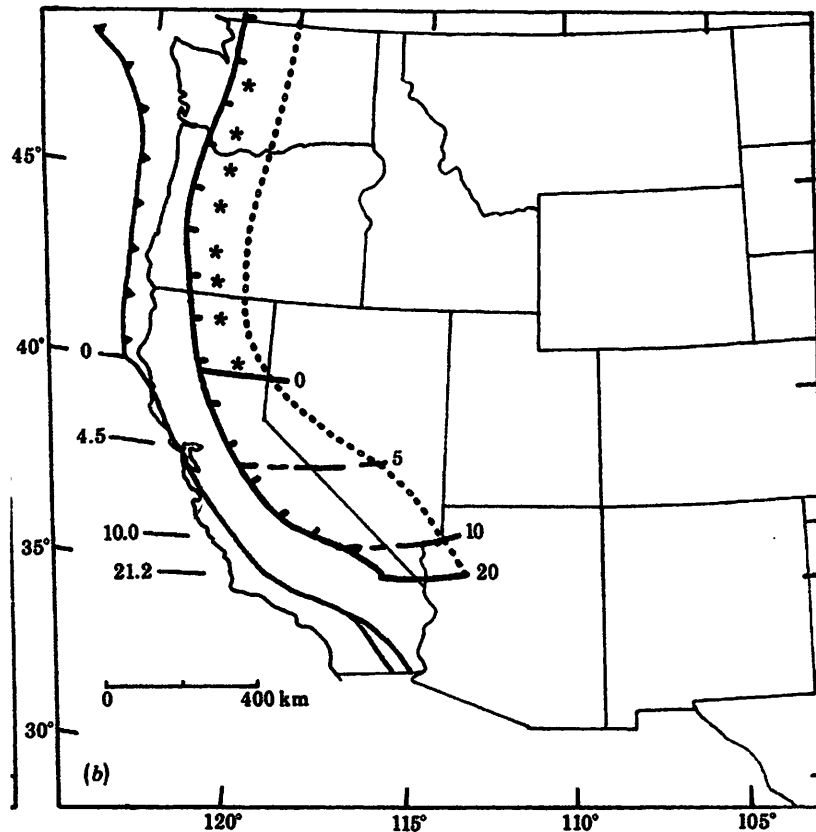


Figure 2: Numbers offshore indicate the northward migration of the triple junction. Numbers inland indicate the southernmost extent of calc-alkaline magmatism. Asterisks represent volcanoes of the Cascade volcanic chain which is the modern volcanic arc. Figure from Zoback *et al.* (1981).

range-bounding faults. The magnitude of this early offset and tilting implies much greater extension than the basin-range faulting event in many areas (Zoback *et al.* 1981). Dyke swarm trends, orientations of uniform fault slip vectors, and the direction of stratal tilt of rocks involved in extensional deformation indicate that in the period of 20-10 Ma the least principal stress orientation was uniformly in the WSW-ENE direction throughout the entire western United States. The processes and mechanisms involved in early extension are difficult to infer, because subsequent deformation has erased much of the evidence of the early extension (Zoback *et al.* 1981).

## 4 Basin and Range Extension

Drilling, stratigraphic and seismic reflexion studies have revealed that angular unconformities in the Southern Basin and Range region developed at about 13 Ma. This is thought to be the beginning of the major block-style graben-forming faulting event which continued to at least 10 and possible 6.5 Ma (Zoback *et al.* 1981). A comparison of the least principal stress orientations at different times suggests that the orientation changed by roughly 45°

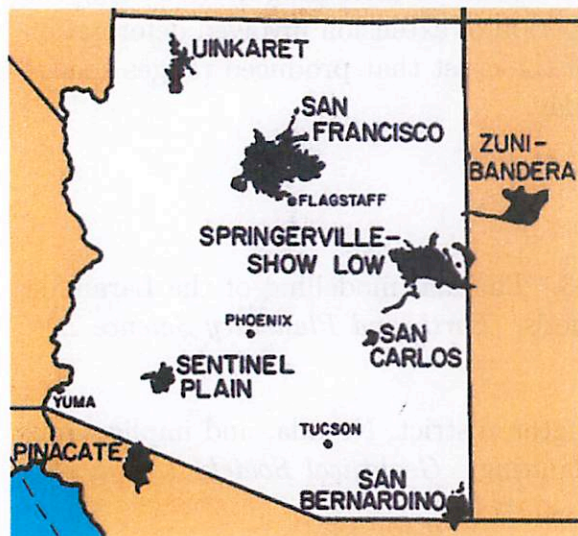
10 Ma. This change in stress orientation was probably caused by (1) elongation of the San Andreas transform to a 'critical' length; (2) acceleration of the relative motion between the Pacific and North American plates; or (3) greater normal stress increasing friction along the San Andreas fault (Zoback *et al.* 1981). This later period of extension involved deformation resulting from block faulting in the upper 15 km of the crust that produced ranges spaced about 25-35 km apart which are easily observed today.

## References

- English, J. M., S. T. Johnston, and K. Wang 2003. Thermal modelling of the Laramide orogeny: testing the flat-slab subduction hypothesis. *Earth and Planetary Science Letters* **214**, 619–632.
- Proffett, J. M. 1977. Cenozoic geology of the Yerington district, Nevada, and implications for the nature and origin of Basin and Range faulting. *Geological Society of America Bulletin* **88**, 247–266.
- Sonder, L. J., and C. H. Jones 1999. Western United States Extension: How the West was Widened. *Annual Review of Earth and Planetary Sciences* **27**, 417–462.
- Thompson, G. A., and D. B. Burke 1974. Regional Geophysics of the Basin and Range Province. *Annual Review of Earth and Planetary Sciences* **2**, 213–+.
- Zoback, M. L., R. E. Anderson, and G. A. Thompson 1981. Cainozoic Evolution of the State of Stress and Style of Tectonism of the Basin and Range Province of the Western United States. *Royal Society of London Philosophical Transactions Series A* **300**, 407–434.

# History of the San Bernardino (Geronimo) volcanic field

PTYS 594, Fall 2009 – Shane Byrne



Field is ~850 Km<sup>2</sup>  
1300m a.s.l.

San Bernardino field shares characteristics with other Arizona volcanics

- Alkali-olivine Basalts (Hawaiite)
- Recent age (0.3 - 3.2 Myr)
- Monogenetic cones (Except stratovolcano at Flagstaff)

## San Bernardino Valley

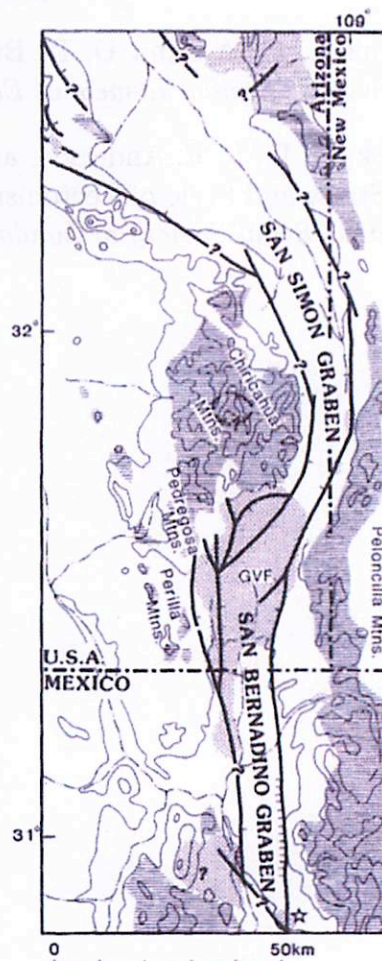
The San Bernardino valley is a classic basin and range graben, bounded on the west by the Chiricahua, Pedregosa and Perilla mountains and on the east by the Peloncilla mountains.

Older Volcanic deposits on bounding mountains show valley has been continuously subsiding.

Valley floor composed of volcanic flows interbedded with alluvial deposits from adjacent mountains. Wells in the valley penetrate 6-7 flows separated by rhyolitic debris washed out of the Chiricahuas. Flows are small, two wells 3km apart penetrate many uncorrelated flows.

The volcanic field occupies northern third of the valley. Tectonics appears to not control vent location (although field is near the contact with the San Simon graben).

Drainage is to the south (Rio San Bernardino) at gradients of 8m/km.



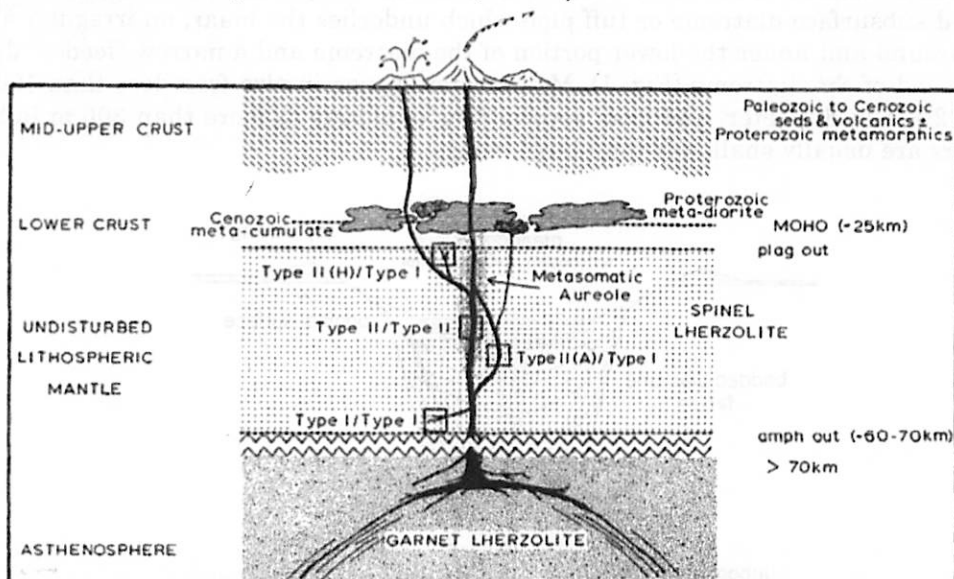


## Volcanic Field

Inventory: Scoria Cones (135)  
Maars (2)  
Other tuff-rings (~3)

Eruptions produced cones of welded splatter. Steam explosions produced Maar craters and tuff-rings. Actual flows are pretty small in extent.

Alkali-Olivine Basalts originate through partial melting of the mantle and rise through the crust without much alteration. Source region thought to be at depths of 67km, local magma chambers ~33km (Evans and Nash, 1968).



Geochemistry ties this field to a fissure eruption (at 0.54 Myr) in Animas valley (tectonically inactive). Flows in San Bernardino are concentrated in the northern valley, away from recent tectonic activity.

Only three samples dated:

Cinder Hill	0.27 Myr
Paramore crater	0.98 Myr (south wall)
Pedregosa mountains	3.30 Myr

## History of San Bernardino valley

- Used to look much like Animas valley – low relief
- Renewed tectonic downdrop of valley floor began > 3 Myr ago
- Valley fills with volcanic flows interspaced with fluviially transported rhyolitic debris

## References

- Lynch, D.J., *The San Bernardino volcanic field of southeastern Arizona*, New Mexico Geol. Soc. Guidbook, 29<sup>th</sup> Field Conf., Land of Cochise, 1978.
- Lynch, D.J., *Neogene volcanism in Arizona: The recognizable volcanoes*, Arizona Geological Society Digest, 17, 681-700.
- Evans, S.H., and W.P. Nash, *Quaternary mafic lavas and ultramafic xenoliths from southeastern Arizona*, Geo. Soc. Amer. Abstracts, vol. 10, 216, 1978.

# Formation of Maar Craters

Patricio Becerra

## Definitions and Physical Characteristics

A maar is a large and shallow volcanic crater cut into pre-eruptive surface. It is essentially the crater of a type of volcanoes known as maar-diatreme volcanoes, which form when hot, rising magma interacts with subsurface groundwater, causing *phreatomagmatic* explosions. These volcanoes consist of the maar crater itself, a ring of tephra surrounding the crater, a cone-shaped subsurface diatreme or tuff pipe which underlies the maar, an irregular-shaped root zone around and under the lower portion of the diatreme and a narrow "feeder" dyke at the bottom end of the diatreme (Fig. 1). Maar craters range in size from less than 100 m to more than 2 km in diameter, and from several tens of meters to more than 300 m in depth. Small maars are usually shallower than large maars.

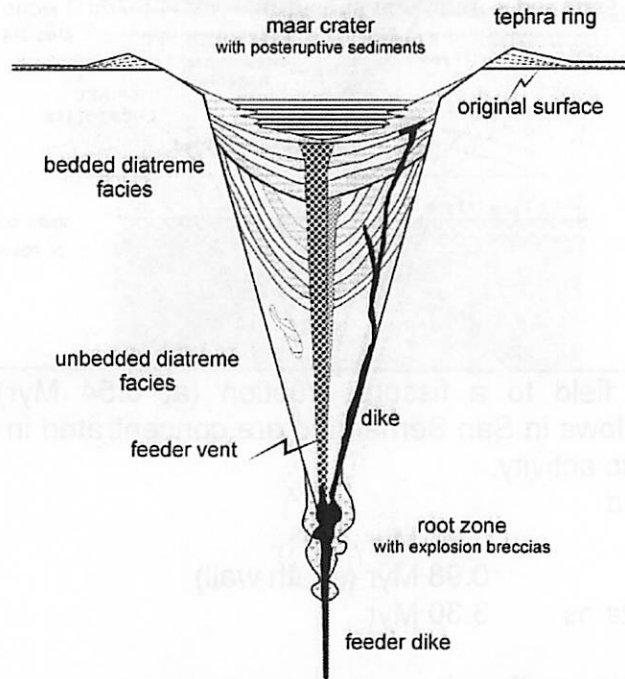


Fig 1. Schematic diagram of a maar-diatreme volcano (Lorenz, 2003).

## Formation of Maar-Diatreme Volcanoes

The formation process of maar diatreme volcanoes (and consequently, of maar craters) has been extensively studied by many scientists since the early 20<sup>th</sup> century, particularly by German geoscientist Volker Lorenz since the early seventies, in whose work is based the bulk of this discussion.

As mentioned above, maar craters form when magma rises and interacts explosively with subsurface groundwater. They do not however, form from one large and fast release of energy like nuclear or impact craters. The energy calculated from diatreme eruptions was found not to be large enough to excavate hard rock walls and form large craters. This means that maar craters have to have been formed by multiple lower-energy explosions over a period of days to months.

The generally accepted theory for the eruption mechanism follows a phreatomagmatic model (*phreatic* = dealing with groundwater, *magmatic* = dealing with magma). When magma of any chemical composition rises through the feeder dike and interacts with stream-water or groundwater in the subsurface, the water is heated quickly and its pressure increases until it finally explodes into steam. As the steam rises toward the surface it ejects rocks and water. At the end of an eruption, the pressure at the source becomes lower than the surrounding lithostatic pressure, which leads to spalling of the wall rocks into the open hole, thus enlarging the initial rupture. The enlarged source fills again with water from above and magma from below, resulting in another explosion. This process repeats itself many times, and the shock waves generated in the explosions create a nearly spherical explosion chamber.

Evacuation of material from in and around the explosion chamber leads to a mass deficiency above the feeder dyke, which in turn results in a downward penetration of the explosion site, forming many interconnected explosion chambers, one below the other (Fig. 2). The total mass deficit of the root zone destabilizes the overlying material. At a certain critical point, the overlying rock collapses into the root zone, pushing the top limit of the root further down. As the explosions themselves push the base of the root downward, like explained above, a cone-shaped sinkhole of subsiding rock is formed. This structure, together with the feeder dyke at the bottom is known as a diatreme.

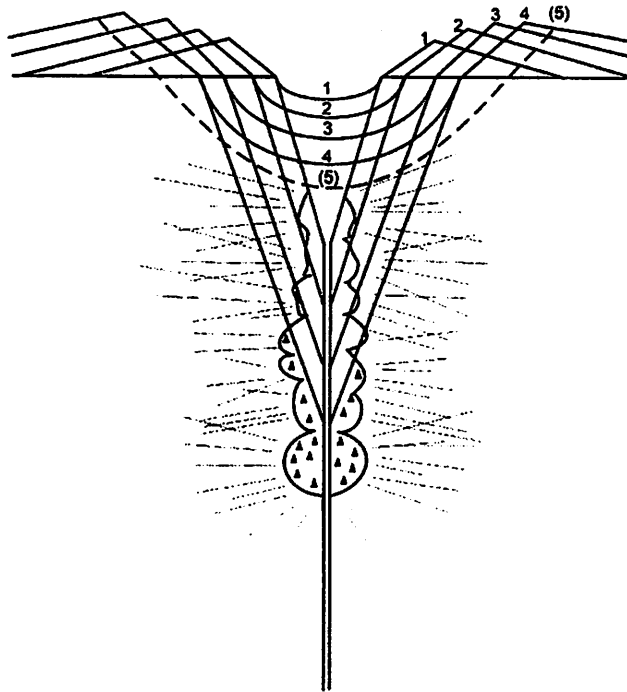


Fig. 2. Schematic of the growth of a maar-diatreme volcano (Lorenz 2003).

As the area of subsidence propagates upward, it eventually reaches the uppermost surface material. The surface is consequently forced to subside and the maar crater is formed. The explosions continue as long as there is sufficient interaction between magma and groundwater. The eruptions and continued collapse phases result in growth of the diatreme and the maar crater.

Maar craters usually have a ring of tephra surrounding them and rising slightly above the surface level. These rings are formed during the eruptions by deposition of ash and volcanic debris through base surges, and range in height from several meters to more than 100 m. If there is a predominant wind direction during the eruptions, the tephra rings will form unevenly, displaying a big lobe in the direction of the wind.

## Differences with other Holes in the Ground

### Impact and Nuclear:

In addition to the longer time and the many low energy bursts it takes to form a maar, physical differences with impact and nuclear craters include flatter floors in maars and much fewer large blocks of debris in the maar deposits.

### Tuff Rings:

Tuff rings have a very similar formation process to maar craters and could even be classified as a type of maar crater. Tuff rings are volcanic structures that form *above* the ground level, whereas maar craters form below ground level and in fact *cut into* the surface.

Tuff rings form when the interaction between magma and groundwater occurs at a very shallow surface level. In this situation there is large amounts of water to refill the explosion chambers, which prevents the significant drops in pressure needed for the walls to burst inward. This reduces the penetration of the root and results in smaller diatremes. The explosions continue, but the material accumulates above the surface faster than the diatreme penetrates downward, resulting in a cone above the surface with a crater in the center, whose floor is in fact at higher elevation than the general surface level (Fig. 3).

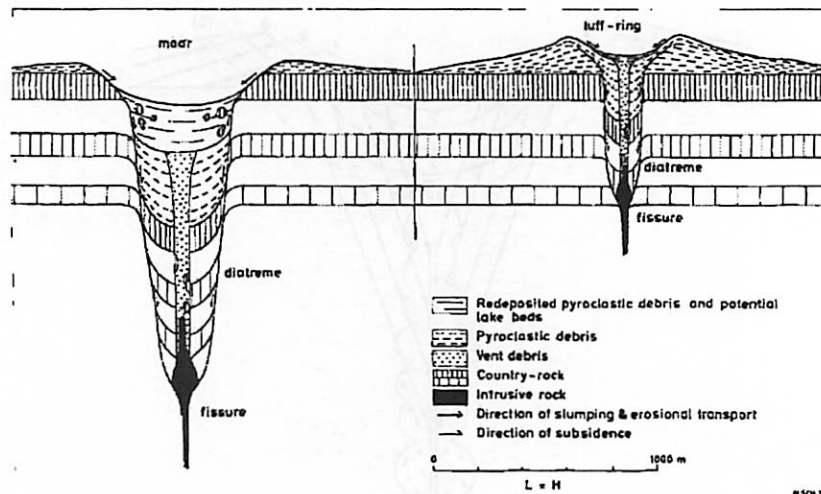


Fig. 3. Differences between maars and tuff rings (Lorenz, 1973).

It is thus accurate to say that Tuff rings form in "special" groundwater rich environments, such as shallow lakes, coastal reefs or alluvial plains. Maar craters in turn, form in more "normal" groundwater environments.

## The Maars in the San Bernardino Volcanic Field

### Characteristics

There are three major maar craters in the San Bernardino or Geronimo Volcanic Field: Paramore Maar, Sotse Maar and Cochise Maar, in order from northeastern-most to southwestern-most crater (Fig. 4).

Paramore maar has an oval shape with a diameter of 1.5 to 2 km. It is about 100 m deep. Sotse crater is very circular and very shallow. Its diameter is about 2 km and its average depth is approximately 20 m. Finally, Cochise maar is smaller than the other two with only a 1 km diameter. It has a 50 m average depth and relatively steep walls.

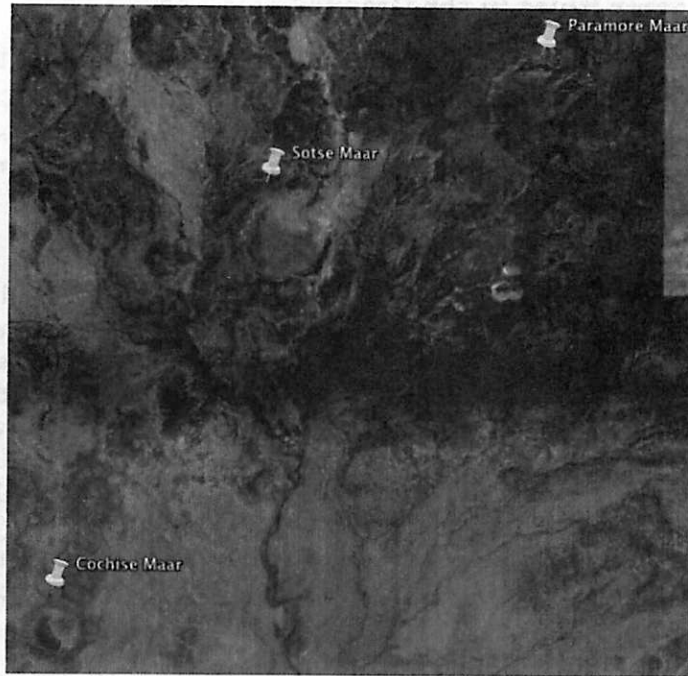


Fig. 4. Satellite image of the maars in the San Bernardino Volcanic Field.

#### Formation Environment

There are two types of groundwater environments in which maar craters can form: groundwater in hard-rock and groundwater in soft-rock environments (Lorenz 2003). The basin and range provinces like the one in the southwestern US consist mainly of soft-rock environments. These environments are made up of unconsolidated sediments, which are water saturated up to very near the surface (which explains the presences of tuff rings in the San Bernardino field). In addition, maars in these environments tend to grow larger than hard-rock maars, due to the much lower strength of the surface material. While it is likely that all maars formed by the phreatomagmatic process described in the previous section, the groundwater environment of the San Bernardino maars allowed them to grow to a larger size than, for example, the hard-rock environment maars in the Eifel region of Germany, which have diameters of less than 1km and are usually filled with water, forming a lake.

#### References

- Lorenz. V. 1973. On the Formation of Maars. *Bulletin of Volcanology* 37: 183-204.
- Lorenz. V. 1986. On the growth of Maars and Diatremes and its Relevance to the formation of Tuff Rings. *Bulletin of Volcanology* 48: 265-274.
- Lorenz. V. 2003. Maar-Diatreme Volcanoes, their Formation, and their Setting in Hard-Rock or Soft-Rock Environments. *Geolines* 15, 72-83.
- Lynch. D. J. 1978. The San Bernardino Volcanic Field of Southeastern Arizona. *New Mexico Geol. Soc. Guidebook, 29<sup>th</sup> Field. Conf., Land of Cochise*, p. 263

# Mantle Nodules and the Bulk Silicate Earth

e.l.berger

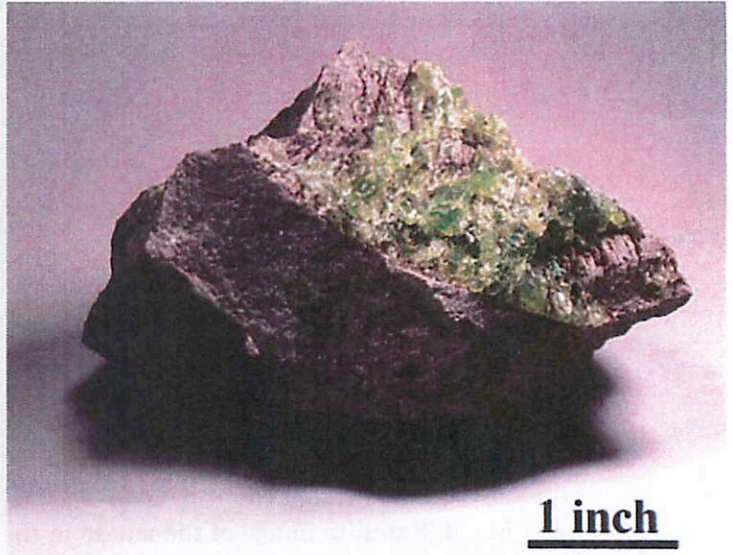
**“Primitive (primordial) mantle is the holy grail of petrology” - C. Herzberg**

The composition of the bulk silicate Earth (or primitive mantle) can provide information about accretion and differentiation processes.

What was the nature of the material accreting to form the Earth? Is it the same material that accreted to form Mars? Venus? Can we approximate the bulk silicate Earth using CI-chondrite abundances?

Mantle nodules are as close as we get to primitive mantle samples. They are fragments of coarse-grained igneous rock, which are crystallized at depth and occur as inclusions in extruded rock.

Worldwide, the most abundant mantle nodules are peridotites. In general this material remains unaltered during transport to the surface, but does not represent primitive material. The bulk and trace element chemistry has been modified by (multiple?) partial melting events, extraction of crustal material, and secondary processing.



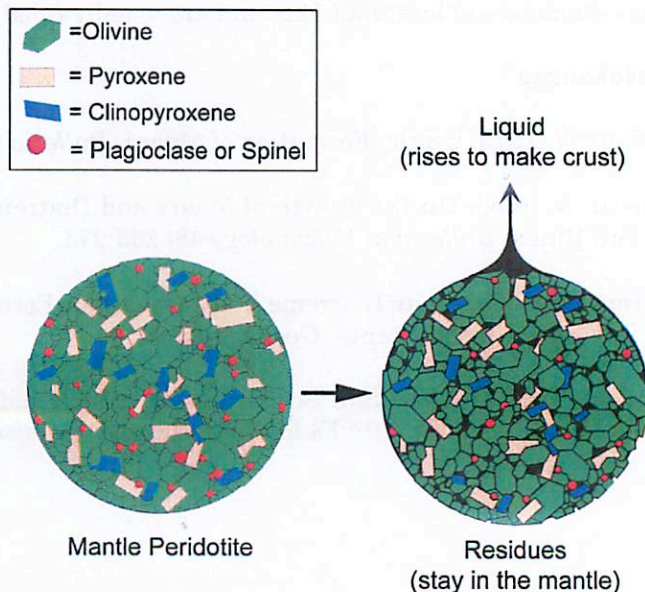
Olivine nodules in basalt. Image from Mt. Lily Gems

**Primordial Mantle – Basalt(s) + Secondary Processing = Residual Peridotite**

*To back out primordial mantle composition, study and model petrologic melt-residue relationships:*

Mantle nodules give direct information on the partial melting of the mantle. Isotopic and chemical analyses of peridotites and basalts allow for the construction of a time-integrated model of mantle evolution.

- Some factors to consider:
- Crystal structures
  - Melting temperatures
  - Elemental incompatibilities
  - Geochemical affinities
  - Pressure effects



Cartoon adapted from C. Herzberg

# Mantle Nodules and the Bulk Silicate Earth

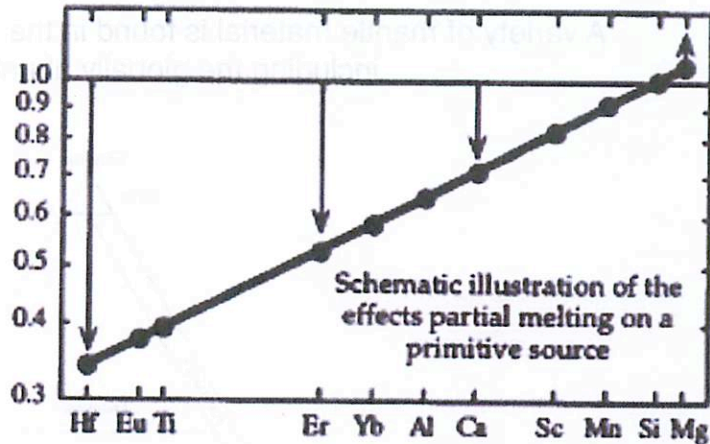
e.l.berger

Which elements are the most incompatible? The relative depletion or enrichment of an element tells us about the type and extent of partial melt extracted.

Partition coefficients allow us to correct back to bulk silicate Earth composition.

Which phases melt first? Which elements are hosted by these phases?

An integration of the answers to these questions (and others) helps to unravel the peridotite's history.



Incompatibility in the crystal decreases to the right. e.g. Hafnium is most incompatible, most depleted in the peridotite, and most enriched in the melt. Figure from McDonough & Sun (1995)

Do the results of melt-residue studies support a CI-chondrite like starting composition?

Cosmochemical Periodic Table of the Elements in the Solar System																							
2.43e10 H																			2.343e9 He <3				
55.47 Li 1342 s	0.7374 Be 1432 s																	17.32 B 900 s	7.079e6 C 40	1.950e6 N 123	1.413e7 O 180	841.1 F 734 s	2.148e6 Ne 9.1
57510 Na 868 s	1.020e6 Mg 1336																	84100 Al 1352 s	1.000e6 Si 1310	8373 P 1229	444900 S 664	5237 Cl 948 s	102500 Ar 47
3692 K 1096 s	62870 Ca 1217	34.20 Sc 1352 s	2422 Ti 1599	288.4 V 1633 s	12860 Cr 1296 s	9168 Mn 1133 s	838000 Fe 1334	2323 Co 1352 s	47800 Ni 1353 s	527 Cu 1037 s	1226 Zn 725 s	35.97 Ga 968 s	120.6 Ge 883 s	6.089 As 1085 s	65.79 Se 697 s	11.32 Br 546 s	55.15 Kr 52						
6.572 Rb 800 s	23.54 Sr 1482 s	4.608 Y 1352 s	11.33 Zr 1171	0.7554 Nb 1352 s	2.601 Mo 1352 s	Tc	1.900 Ru 1352 s	0.3708 Rh 1352 s	1.435 Pd 1324 s	0.4913 Ag 986 s	1.584 Cd 652 s	0.1810 In 536 s	3.733 Sn 704 s	0.3292 Sb 979 s	4.815 Te 709 s	0.9975 I 535 s	5.391 Xe 68						
0.3671 Cs 799 s	4.351 Ba 1432 s	0.4405 La 1352 s	0.1699 Hf 1352 s	0.02099 Ta 1352 s	0.1277 W 1788 s	0.05254 Re 1621 s	0.6738 Os 1812 s	0.6448 Ir 1604 s	1.357 Pt 1498 s	0.1958 Au 1060 s	0.4128 Hg 252 s	0.1845 Tl 532 s	3.258 Pb 727 s	0.1388 Bi 748 s	Po	At	Rn						
Fr	Ra	Ac	Rf	Ha	106	107	108	109	110	111	112												
K. Lodders, 2003, Solar System Abundances and Condensation Temperatures of the Elements, <i>Astrophys. J.</i> 591, 1220-1247		1.169 Ce 1432 s	0.1737 Pr 1352 s	0.8355 Nd 1352 s	Pm	0.2542 Sm 1352 s	0.09513 Eu 1352 s	0.3321 Gd 1352 s	0.05907 Tb 1352 s	0.3862 Dy 1352 s	0.08986 Ho 1352 s	0.2554 Er 1352 s	0.0370 Tm 1352 s	0.2484 Yb 1352 s	0.03572 Lu 1352 s								
		0.03512 Th 1352 s	Pa	9.31e-3 U 1352 s	Np	Pu	Am	Cm	Bk	Cf	Es	Fm	Md	No	Lr								

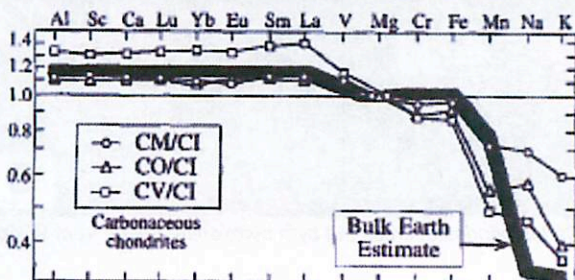


Figure from McDonough & Sun (1995)

Bulk Earth and CI-chondrite abundances of refractory and common lithophile elements are similar, but the Earth is much more depleted in volatiles.

There is no meteoritic bulk composition that matches the Earth.

# Mantle Nodules and the Bulk Silicate Earth

e.l.berger

## Depletion & enrichment events under the Geronimo Volcanic Field

A variety of mantle material is found in the Geronimo Volcanic Field (GVF), including the globally abundant peridotites.

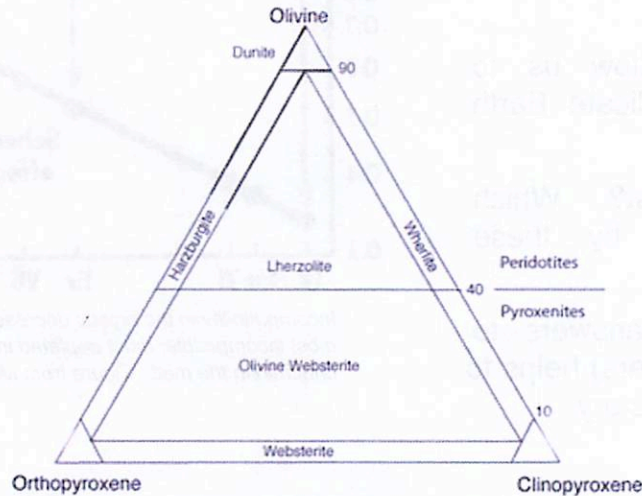


Image from Wikipedia

In particular, the GVF has Cr-diopside containing spinel lherzolites & harzburgites.

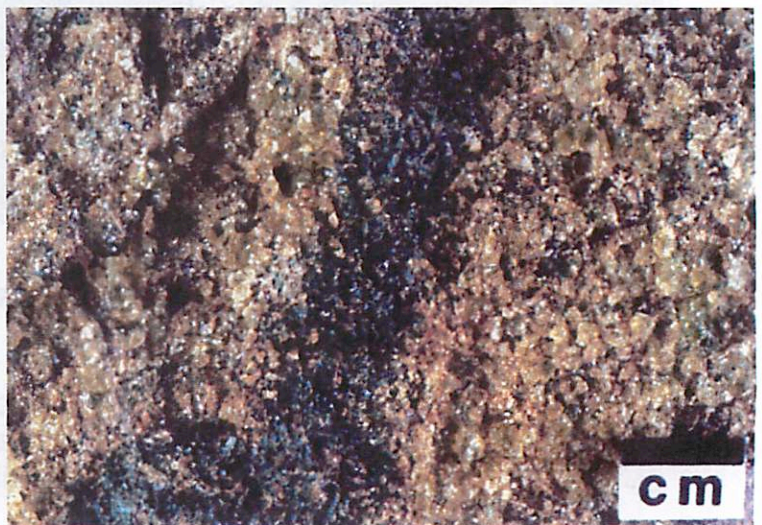
- some are rare earth element depleted
- some are rare earth element enriched
- some contain hydrous accessory minerals
- some contain anhydrous accessory minerals

The GVF also has Al- & Ti-augite clinopyroxenites.

Mantle material under the GVF has been depleted to various degrees by partial melting and extraction of crustal material, and then enriched (or depleted) by secondary processes (e.g. interaction with silicate melts, or hydrous fluids).

### Proposed History:

- Early depletions during continent formation
- Rare earth element enrichment (relatively recent)
- Infiltration of water and silicate melts: rare earth element depletions



San Carlos peridotite, cross-cut by a pyroxenite. Image from Wikipedia

46



# Mantle Nodules and the Bulk Silicate Earth

e.l.berger

## Terminology

Igneous: solidified from molten or partly molten material

Olivine: isolated silica ( $\text{SiO}_4$ ) groups

Fayalite ( $\text{Fe}_2\text{SiO}_4$ )

Forsterite ( $\text{Mg}_2\text{SiO}_4$ )

Orthopyroxene (opx): single chain silicates

Ferrosilite ( $\text{FeSiO}_3$ )

Enstatite ( $\text{MgSiO}_3$ )

Clinopyroxene (cpx): single chain silicates

Ca- and Al-bearing pyroxenes,

Diopside ( $\text{CaMgSi}_2\text{O}_6$ )

Augite (garbage-can pyroxene:  $(\text{Ca},\text{Na})(\text{Mg},\text{Fe},\text{Al})(\text{Si},\text{Al})_2\text{O}_6$ )

Plagioclase feldspar: framework silicates

Albite ( $\text{NaAlSi}_3\text{O}_8$ )

Anorthite ( $\text{CaAl}_2\text{Si}_2\text{O}_8$ )

## Spinel

An isomorphous series of oxides

$(\text{Mg},\text{Fe},\text{Zn},\text{Mn})\text{Al}_2\text{O}_4$

Peridotite: low Fe- olivine +/- pyroxenes +/- minor plagioclase +/- minor spinel

Iherzolite Spinel: olivine plus two-pyroxene peridotite (opx & cpx)

Harzburgite: olivine and orthopyroxene (forms from partial melt of Iherzolite)

## Geochemical

lithophile: rock-loving

siderophile: metal-loving

chalcophile: sulfur-loving

atmophile: gas-loving

## Cosmochemical

refractory

common

volatile

highly-volatile

$T_c \geq 1400^\circ\text{C}$

$T_c$  between  $\sim 1350$ - $1250^\circ\text{C}$

$T_c$  between  $\sim 1250$ - $800^\circ\text{C}$

$T_c \leq 800^\circ\text{C}$

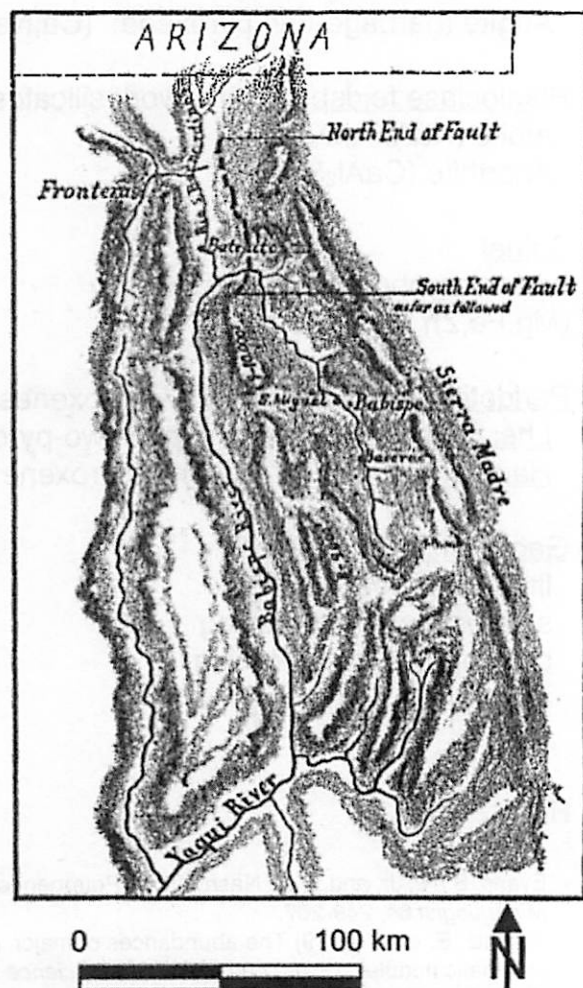
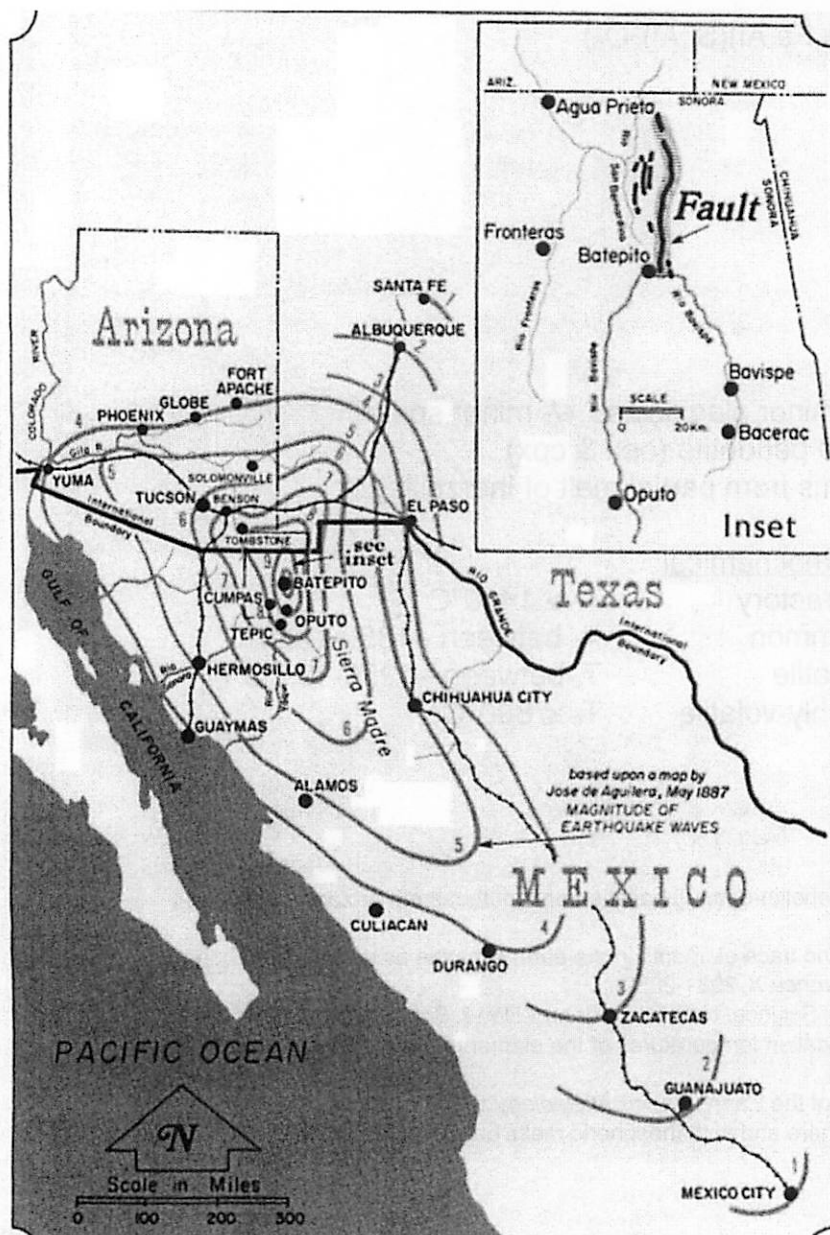
## References

- Evans, S. H., Jr. and W. P. Nash (1979) Petrogenesis of xenolith-bearing basalts from southeastern Arizona. *American Mineralogist* 64, 249-267.
- Jagoutz, E. *et al.* (1979) The abundances of major, minor and trace elements in the earth's mantle as derived from primitive ultramafic nodules. *Proc. Lunar Planetary Science Conference X*, 2031-2050.
- Klein, C. (2002) The 22nd Edition of the Manual of Mineral Science. New York: John Wiley & Sons, Inc.
- Lodders, K. (2003) Solar system abundances and condensation temperatures of the elements. *Astrophysical Journal* 591, 1220-1247.
- McDonough, W.F. and S.-s. Sun (1995) The Composition of the Earth. *Chemical Geology* 120, 223-253.
- Menzies, M. *et al.* (1984) Interaction of continental lithosphere and asthenospheric melts below the Geronimo Volcanic Field, Arizona, USA. *Journal of Petrology* 26, 663-693.

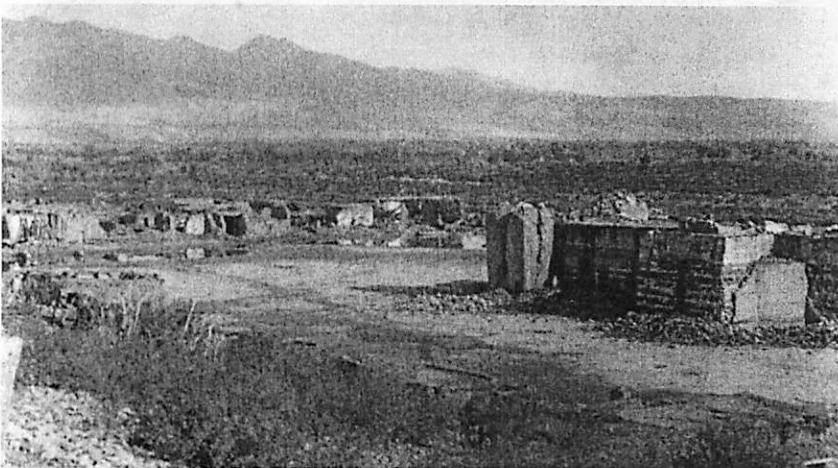
## The Great Sonoran Earthquake of 3 May 1887 by David Choi

On the afternoon of May 3, 1887, a strong (estimated magnitude of 7.5) earthquake struck northern Sonora, Mexico. Seismic activity and ground shaking was reported by citizens from all over Mexico and the Southwestern US. The earthquake resulted in 51 deaths, numerous injuries, and widespread property damage. Though this seismic event occurred before the era of widespread scientific instrumentation, some citizens from the era led the charge to measure and document as much of the earthquake's effects as possible.

Left: Modern reproduction of a map originally drawn by Jose de Aguilera, May 1887. (Bennett, 1977). Right: Sketch map of the rupture trace by George Goodfellow in 1887 (Suter, 2006)



▲ Figure 3. Sketch map of the rupture trace by Goodfellow (1887b), who mapped the surface rupture in the south ~8 km beyond its intersection with the Bavispe River. The rupture trace mapped by Goodfellow as well as Aguilera (Figure 5) has an end-to-end length of 56 km and is now known as the Pitáycachi segment of the surface rupture. The scale is approximate.

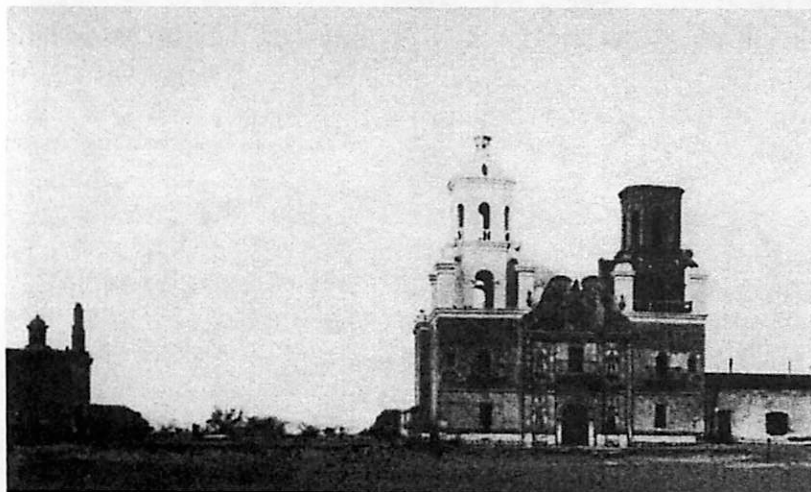


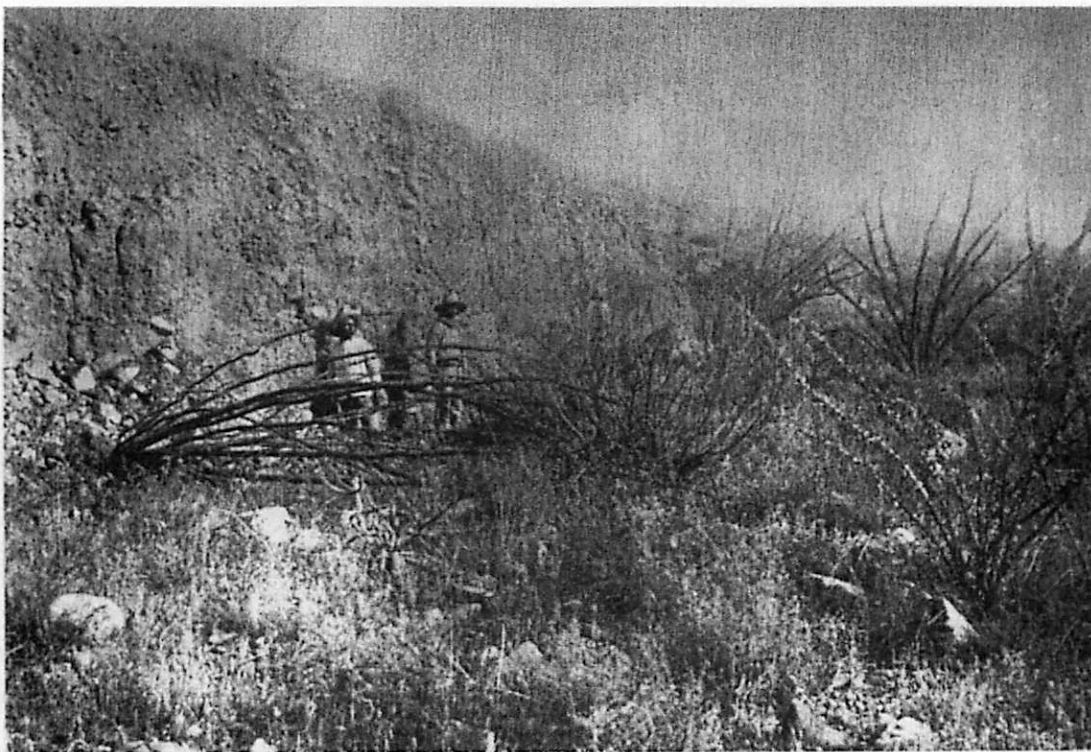
Top: The church in Bavispe, Sonora, after the 1887 earthquake. A large majority of the earthquake's fatalities occurred here, when panicked citizens fled to the church during the quake, only to have the building eventually collapse.

Middle: The town of Bavispe, Sonora, after the quake.

Bottom: Mission San Xavier south of Tucson, 1902. The structure escaped relatively unharmed, though this picture documents a brick wall fence to the left that was knocked down during the quake.

Source: Bennett, 1977

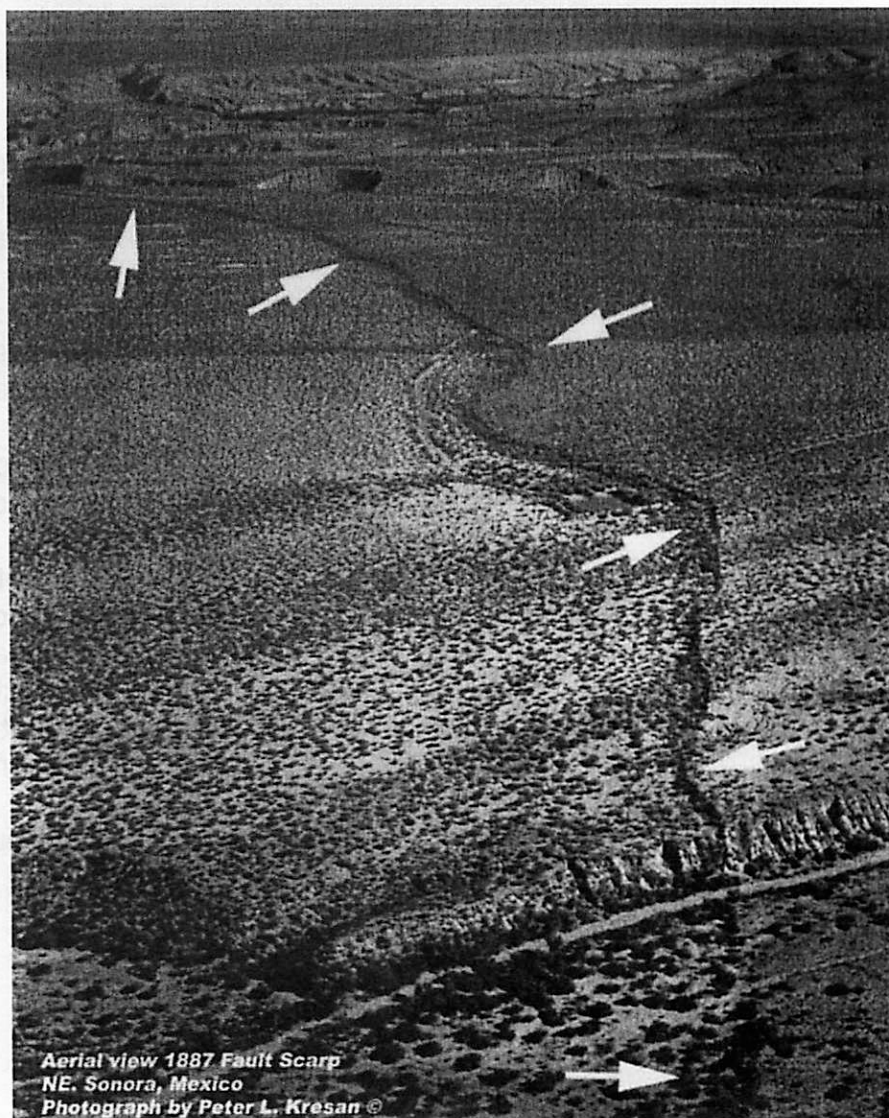




▲ **Figure 6.** Previously unpublished 1887 photograph by Camillus S. Fly of the earthquake rupture scarp in an ocotillo forest between Arroyo Pitáycachi and Cañón de los Embudos, most likely at 109.135 long. W / 31.088 lat. N. (Figure 2). The view is from the northwest. The scarp is subvertical, composed of alluvial gravel cemented by caliche, and its height is estimated here as ~4.4 m. The two persons are standing in a fissure or crevice that developed along the scarp. The ground surface is not rotated toward the scarp, which suggests a simple planar near-surface geometry of the rupture.

Top: Portion of the fault scarp photographed in 1887. Note the scale of the vertical relief in the scarp relative to the people captured in the photograph.  
Source: Suter, 2006

Right: Aerial view of the fault scarp in the San Bernadino Valley in NE Sonora, Mexico.  
Source: Bennett, 1977



Aerial view 1887 Fault Scarp  
NE. Sonora, Mexico  
Photograph by Peter L. Kresan ©

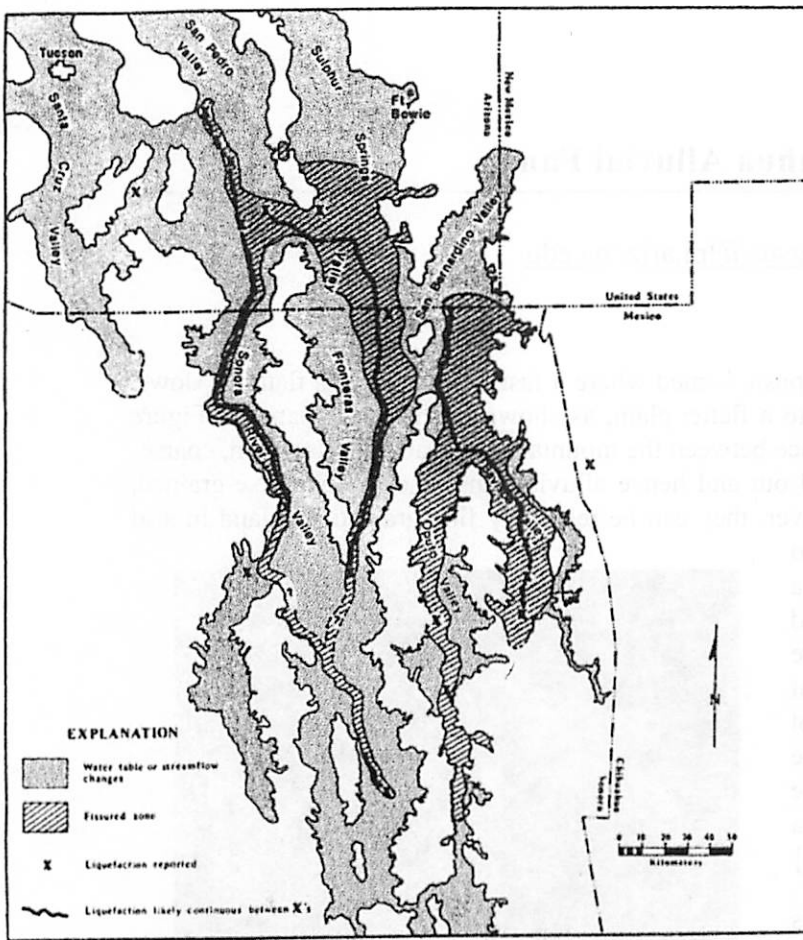


Figure 5. Liquefaction, ground fissures and hydrologic alterations associated with the May 3, 1887 earthquake in Sonora, Mx. (from DuBois and Smith, in press)

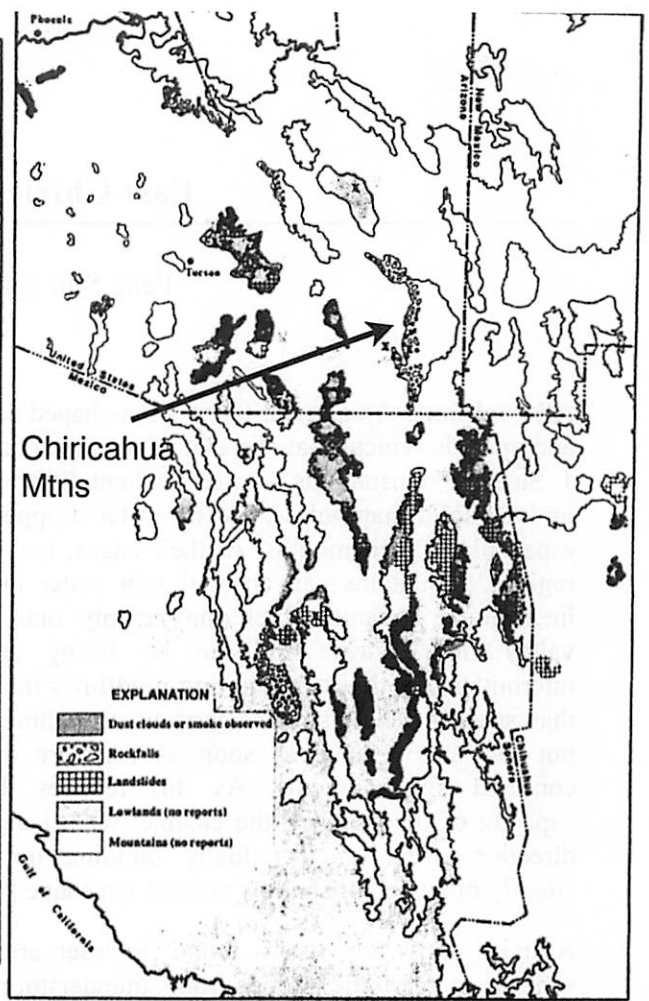


Figure 6. Mass movement induced by the 1887 earthquake in Sonora. "X's" indicate specific locations named in rockfall or landslide reports (from DuBois and Smith, in press).

Left: Map of ground/hydrological effects from the Sonora earthquake. Grayscale dotted areas indicate water table/streamflow changes, slanted hash lines indicate ground fissures, and X's mark reports of soil liquefaction. Right: Map of mass movement effects from the Sonora earthquake. Grayscale dots indicate observed dust clouds or smoke, small outlines of irregular shapes indicate rockfalls, a grid pattern indicates landslides, and outlines indicate lowlands and mountains with no reports. Source: Dubois and Smith, 1980

**Bibliography**

An extensive collection of literature has been collected online, complete with PDFs and links to a large fraction of the original literature. It is located at <http://www.geo.arizona.edu/gsat/1887eq/bibliography.html>

Bennett, E.F., "An afternoon of terror: The Sonoran earthquake of May 3, 1887," *Arizona and the West, A Quarterly Journal of History*, H.P. Hinton, ed. **19**(2): 107-120, 1977.

DuBois, S. M., and A.W. Smith, "The 1887 Earthquake in San Bernardino Valley, Sonora: Historic accounts and intensity patterns in Arizona," *Univ. Ariz. Bur. Geol. Min. Tech. Special Paper No. 3*. 1980

Suter, M. "Contemporary studies of the 3 May 1887 Mw 7.5 Sonora, Mexico (Basin and Range Province) earthquake," *Seismol. Res. Letters*, **77**(2): 134-147, 2006.

## East Chiricahua Alluvial Fans

Peng Sun [pengsun@lpl.arizona.edu](mailto:pengsun@lpl.arizona.edu)

**Alluvial fans:** An alluvial fan is a fan-shaped deposit formed where a fast flowing stream flattens, slows, and spreads typically at the exit of a canyon onto a flatter plain, as shown in the upper panel in Figure 1. Since there usually is marked gradient difference between the mountain slope and the flat plain, coarse-grained solid material carried by water dropped out and hence alluvial fans tend to be coarse-grained, especially at their mouths. At their edges, however, they can be relatively fine-grained. On land in arid regions, mountains can channel rain water into intermittent streams which may empty onto a valley floor. Flow tends to be flashy and intermittent, at times resembling mudflows more than streams. These streams carry much sediment but lose competence as soon as they are not confined by mountains. As this reduces the capacity of the channel, the channel will change direction over time, gradually building up a slightly mounded or shallow conical fan shape.[1]

Alluvial fans are often found in desert areas subject to periodic floods from thunderstorms nearby. They are common around the margins of the sedimentary basins of the Basin and Range states of southwestern North America. The typical water course in an arid climate has a large, funnel-shaped basin at the top, leading to a narrow defile, which opens out into an alluvial fan at the bottom. Multiple braided streams are usually present and active during water flows on parts of the fans as shown in the bottom panel in Figure 1.

The deposits are usually poorly-sorted. Suppose the solids are sorted as usual, with coarse sediment dropped out first, but the sorting of an individual flood event is then "jumbled" by the next flood (as the flood is flash and intermittent), leaving the overall fan sediment package poorly-sorted.

Figure 3 shows an erosion-deposition process that transfers material between an upland and adjacent basin in arid area as sediment. Sediment from erosion within the mountains is moved by these distributaries to the adjacent basin. In arid and semiarid regions, this is either an irregular or seasonal process driven by strongly seasonal rainfall or rapid snowmelt. Sediment transfer is thus frequently associated with intermittent flash floods that may include mudflows. The fans, the main sites of



**Figure 1:** The upper panel shows an alluvial fan coming out of a canyon. The bottom panel shows an alluvial fan with active distributaries (left fan region) flowing partly.

deposition, therefore formed an intrinsic part of an erosional-depositional system in which mountains tend slowly to wear away and basins to fill with sediment through geologic time.[2]

### Alluvial Fans on Mars?

Since the alluvial fans are associated with mountains, basins and distributaries, the identification of alluvial fans on other planets would indicate fluvial features. Figure 3 shows a possible alluvial fan on Mars. A separate alluvial fan (Image 2) is found near the southwestern corner of Holden crater. The wind has stripped away the finer sediment that once covered much of this fan surface, leaving many of the old stream bed deposits standing in positive relief. The long channels, wind erosion, and low gradients of these fans suggest deposition mostly by normal stream flows rather than debris flows.[3][4]

There have been also some features on Mars

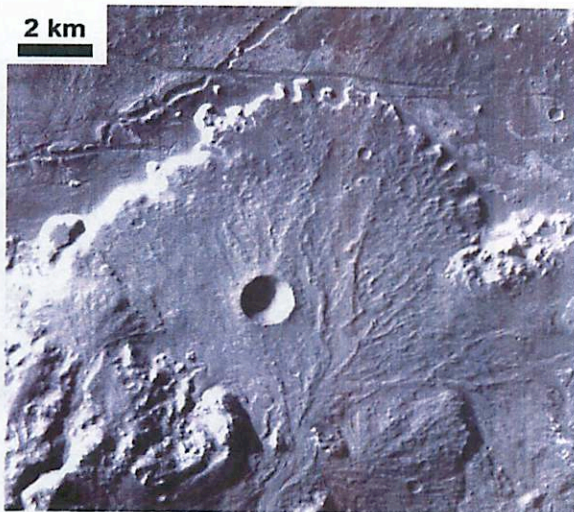


**Figure 3:** A large alluvial fan in the southern floor of Holden crater, showing inverted (positive-relief) distributary channels that were preserved while wind stripped away fine-grained sediment between them. THEMIS visible imaging, 17 m/pixel.

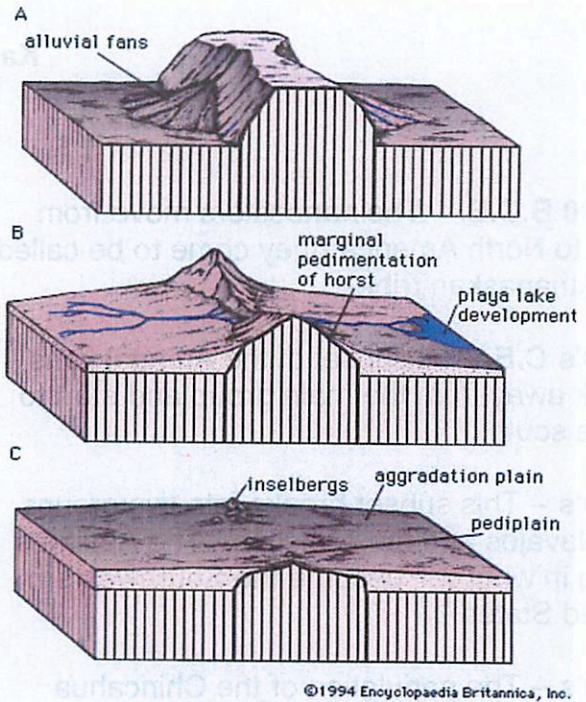


**Figure 2:** An erosion-deposition process that transfers material between an upland and adjacent basin in arid area as sediment by distributaries over the alluvial fans.

interpreted as delta (Figure 4), the transitional depositional interface between the stream and marine environments. Also it has a coarsening upward sequence resembling alluvial fans. However, the alluvial fans would have relatively poorer sorted arrangement and coarser material at the mouth as the flows are intermittent.

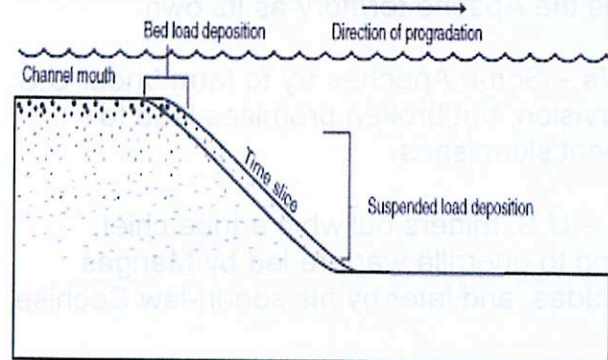


**Figure 4:** The intersection of a delta.

**Reference:**[1]Wikipedia[2]Encyclopedia Britannica[3]Kraal, E. R et al (2008), Catalogue of large alluvial fans in martian impact craters, Icarus, 194, 101-110 [4]Moore, J. M. et al (2005), Large alluvial fans on Mars, J. Geophys. Res., 110, E04005

## A Brief History of the Chiricahua Native Americans

Kat Volk

**~1000 B.C.E.** – Their ancestors move from Asia to North America (they come to be called the Athapaskan tribe).

**1300's C.E.** – A subset of the Athapaskans break away from the main group and start to move south.

**1400's** – This subset breaks into two groups, the Navajos and the Apaches. The Apaches settle in what will become the Southwestern United States.

**1600's** – The population of the Chiricahua Apaches has grown to about 3000.

**1700's** – The Apaches push south into Mexico and encounter the Spanish. A mixture of raiding and trading commences.

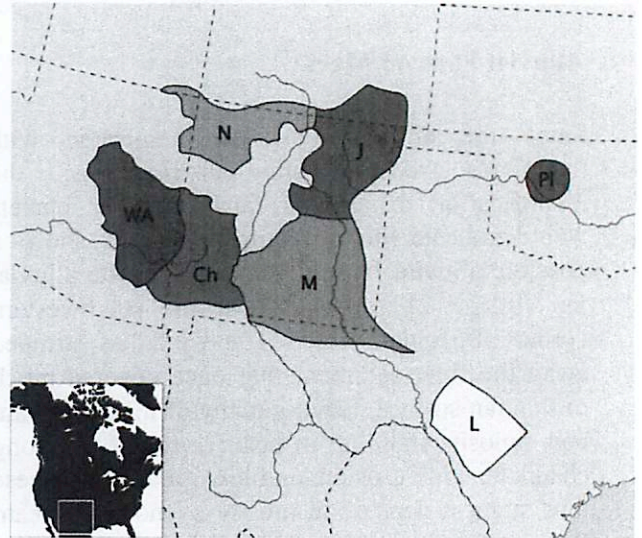
**1821** – Mexico places a bounty on Apache scalps, escalating the existing violence.

**1848** – Mexico and the U.S. are at war, and the Apaches help the U.S. by continuing their violence against Mexico. After the war the U.S. claims the Apache territory as its own.

**1850's** – Some Apaches try to farm under U.S. supervision, but broken promises lead to frequent skirmishes.

**1861** – U.S. miners bullwhip a tribe chief, leading to guerrilla warfare led by Mangas Coloradas, and later by his son-in-law Cochise.

**1863** – Mangas Coloradas is killed by the U.S. army while attempting to sue for peace.



**18<sup>th</sup> century tribal lands** (WA = Western Apache, N = Navajo, Ch = Chiricahua, M = Mescalero, J = Jicarilla, L = Lipan, PI = Plains Apache)

Source: Goddard, Ives. (1999). Native languages and language families of North America



**Mangas Coloradas** (date unknown)

source: [http://es.wikipedia.org/wiki/Mangas\\_Coloradas](http://es.wikipedia.org/wiki/Mangas_Coloradas)





**Geronimo (Goyahkla)**

source:

<http://en.wikipedia.org/wiki/File:Goyaale.jpg1>

**1874** – Cochise surrenders, but separate bands of Apaches continue the raiding.

**1870's** – The Apaches are forced onto the San Carlos Reservation.

**1881** – Geronimo (also known as Goyahkla) leads a group of Apaches away from the reservation.

**1883** – Geronimo and followers return peacefully to the San Carlos Reservation.

**1885** – Geronimo and company again leave the reservation over the banning of a ceremonial drink.

**1886** – Geronimo surrenders in Mexico, but then escapes on the way back to the U.S. Several months later Geronimo again surrenders, signaling the end of Apache warfare against the U.S. As a punishment the Chiricahuas are sent to prison in Alabama and Florida.

**1894** – The Chiricahuas who have not died in prison are sent to a reservation in Oklahoma.

**1909** – Geronimo dies as a prisoner of war.

**1913** – The Chiricahuas are granted freedom.



Geronimo's camp in April 1886, one month before his final surrender.

source: [http://en.wikipedia.org/wiki/File:Geronimo\\_camp\\_17apr1886.jpga](http://en.wikipedia.org/wiki/File:Geronimo_camp_17apr1886.jpga)

# Clovis culture and megafauna extinction, the Big Freeze, and a Giant Impact

by Serina Diniega

The Clovis culture<sup>i</sup> was the earliest well-established human culture in the North American continent, although they were probably not the first people in the American continents. They were hunters of big-game – the culture is named after the town Clovis, NM, where the first example of a Clovis point (Fig. 1) was found with butchered mammoth remains in the 1930s. Clovis archaeological sites are dated to around 13 kyr BP.

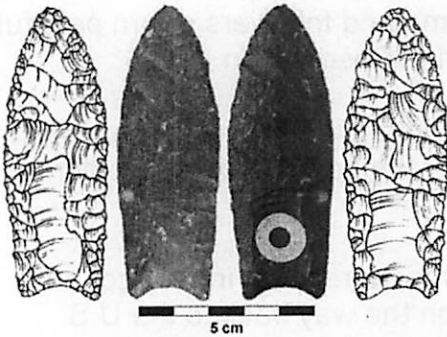


Fig. 1<sup>ii</sup>: Clovis points are thin, fluted projectile points created using bifacial percussion flaking applied to flint, chert, jasper, or other stones of conchoidal fracture. Clovis points are characterized by concave longitudinal grooves on both faces, 1/3 or more up from the base to the pointed tip, which may have been used to fasten the points to spears or shafts. They have been found throughout N. America and south to Venezuela.<sup>iii</sup>

The Clovis culture lasted 200-800 yr – it is thought that the end of the Clovis culture is due to a decline in the availability of megafauna (at least 35 mammal and 19 bird genera disappeared). It was originally hypothesized that overhunting drove the mammoth and other species to extinction (the *Pleistocene overkill hypothesis*). A currently more accepted idea is that an abrupt cooling (the *Younger Dryas* or *Big Freeze*, a cold climate period 11-10 kC<sup>14</sup>yr ~ 12.9-11.5 kyr BP) during the *Late Glacial Maximum* was the main cause of the extinction.

A geological marker of the *Younger Dryas* climatic episode is an organic-rich layer of soil called *sapropelic silt*, *peaty muds*, *paleo-aquolls*, or *black mat* that has been found globally and dated to ~ 12.9 kyr BP.<sup>iv</sup> This distinct layer was first connected with the end of the Clovis culture at Murray Springs, where excavations were conducted by UA professor C. Vance Haynes in the 1960s. The Clovis occupation surfaces were found in place, directly beneath the *Clanton Clay deposit* (AKA the *black mat*).<sup>v</sup>

*Black mats* have been identified at 70 other Clovis sites (Fig. 2), each with similar dates and stratigraphic position.<sup>vi</sup>

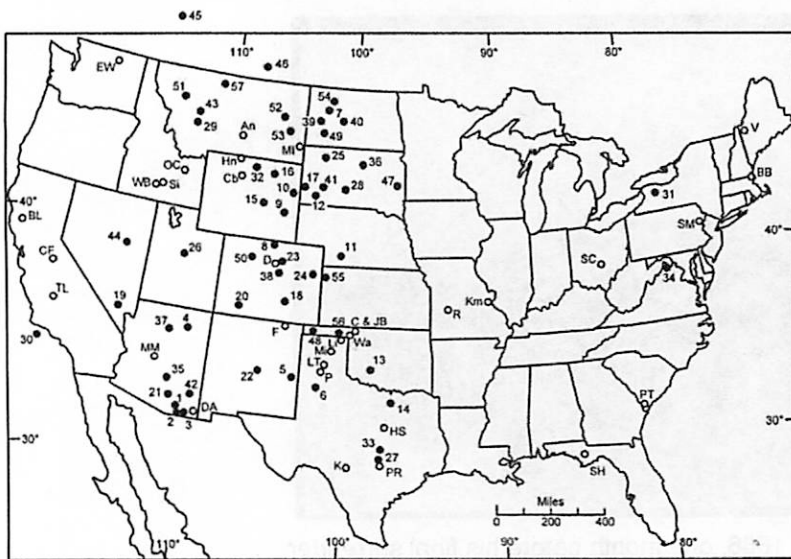


Fig. 2<sup>vi</sup>: Map showing locations where one or more Clovis sites contain overlying black mats of Younger Dryas age (filled circles), and 27 localities with Pleistocene-Holocene transitional sediments but no black mats (open circles).

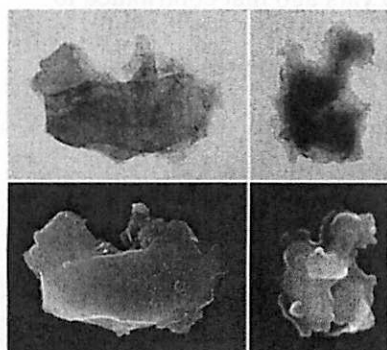
The coincidence between the *black mat*, the decline of the Clovis culture, the extinction of megafauna, and the sudden onset of the Younger Dryas have led scientists to search for a “triggering event” – such as an extraterrestrial impact.<sup>vii</sup> An impact event could have created a devastating, high-temperature shock wave and initiated extensive, extreme wildfires. Ozone depletion and the atmospheric injection of sunlight-blocking chemicals, water vapor, and soot could have contributed to cooling. Additionally, long-term (~1000yr) cooling could result from impact-related destabilization or melting of the ice sheet, disrupting the thermohaline circulation.

At 10 Clovis or Clovis-age sites, a 3cm-thick sediment layer beneath the *black mat* (12.9 kyr BP) was found to contain signatures of an extraterrestrial impact and increased wildfires (Tab. 1). This evidence points towards a carbon-rich, nickel/iron-poor impactor (such as a comet) which experienced fragmentation, a hypervelocity oblique impact into a low-impedance surface (such as the Laurentide Ice sheet) or an airburst explosion -- thus leaving no large crater.

Clovis-age YDB Sites	Date, ka	Misc. markers	Carbon	Magnetic microspherules			Magnetic grains				Bulk		
			Spherules #/kg	#/kg	FeO, %	TiO <sub>2</sub> , %	g/kg	H <sub>2</sub> O	FeO, %	TiO <sub>2</sub>	Ni, ppm	IrM, ppb	IrB, ppb
Gainey, MI	~12.4	AGC	1,232	2,144	41	25	3.2	3.2	14	1.6	54	<2	<0.5
Murray Springs, AZ	12.99	AKGCFPSB	0	109			2.6	5.1	21	16	40	<1	2.3
Blackwater Draw, NM	12.98	AKGCFPB	0	768	56	33	2.1	1.5	27	8.1	256	24	2.3
Chobot, AB	~13	AGCB	11	578			1.9	5.0	14	0.9			
Wally's Beach, AB	12.97	AK	—	6			7.8	1.6	41	8.3	190	51	<1
Topper, SC	<13.5	AG	2	97			1.1	0.7	25	49	440	2	<1
Lommel, Belgium	12.94	ACB	0	16	14	67	0.8	0.8	23	21	23	117	<1
Morley Drumlin, AB	~13	GCB	16	1,020	60	29	9.9	3.7	14	1.4	240	<0.1	
Daisy Cave, CA	13.09	GCFPB	>0	>0			>0						<1
Lake Hind, MB	12.76	GCB	184	0			0.3						3.8
Carolina Bays, Min		GCFB	142	20			0.5	0.3	18	21		<1	0.5
Carolina Bays, Max		GCFB	1,458	205			17	1.3	26	34	<200	15	3.8

Table 1<sup>vii</sup>: Radiocarbon ages are calibrated. Percentages are by weight. A, artifacts from Clovis or contemporaries; K, megafaunal kill-site; G, glass-like carbon; C, charcoal; F, fullerenes with ET He-3; S, soot; P, polycyclic aromatic hydrocarbons; B, black mat; Ni, nickel in magnetic fraction; IrM, Ir in magnetic fraction; IrB, Ir in bulk sediment. No measurable Ir was found outside the YDB.

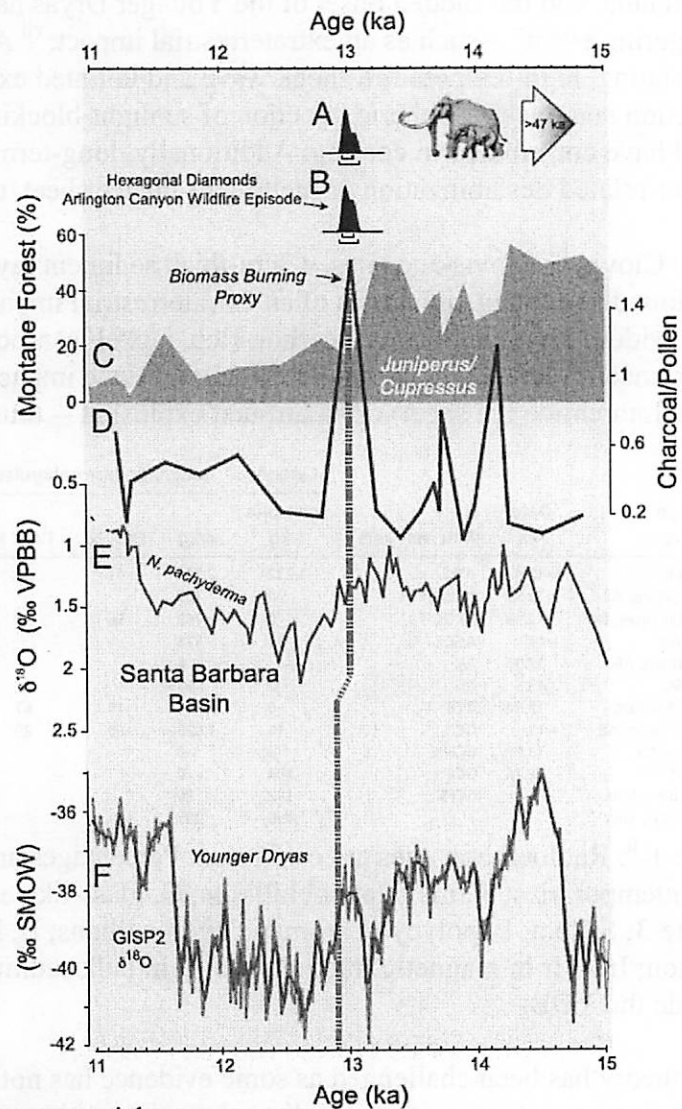
This theory has been challenged as some evidence has not been replicated (such as the helium-rich fullerene and concentrated iridium detection) or has possibly been misinterpreted (such as the magnetic microspherules).<sup>viii,ix</sup> The soot has been tied to increased fires, but these may be due to the rapid climate change, not a catastrophic impact.<sup>x</sup> The primary remaining point of contention is the existence of nanodiamonds: an early study using carbon-13 nuclear magnetic resonance claimed to find nanodiamonds<sup>xi</sup>, but experts disagreed.<sup>ix</sup> A recent study using transmission electron microscope found shock-synthesized hexagonal nanodiamonds



(lonsdaleite) in sediments dating to 12.95 kyr BP from Santa Rosa Island, CA. These lonsdaleite crystals (associated with meteorites and impact craters) were also found with n-diamonds (associated with TNT explosions and meteorites) and cubic diamonds (which are also found at K/T boundary sites).<sup>xii</sup>

Fig. 3<sup>xii</sup>: Transmission electron microscope photomicrographs (top) and scanning electron microscope images (bottom) of 2 stacked diamond clusters, composed primarily of lonsdaleite crystals from the 12.95 kyr BP sedimentary layer.

Fig. 4<sup>xii</sup>: Comparison of the known terminal age of *Mammuthus exilis* with (A) the age of Arlington Canyon hexagonal diamonds, (B) large soot concentration, (C) percent abundance of montane forest types (*Juniperus-Cupressus*), (D) ratio of charcoal/pollen concentration, (E)  $\delta^{18}\text{O}$  record of *Neogloboquadrina pachyderma* (planktonic foraminifera), and (F) Comparative Greenland Ice Sheet  $\delta^{18}\text{O}$  record. Heavy gauge lines represent splines of raw data. The vertical Gray dashed line marks the initiation of the Younger Dryas cooling event in Greenland and Santa Barbara Basin, an event considered synchronous between these records.



<sup>i</sup> [http://en.wikipedia.org/wiki/Clovis\\_culture](http://en.wikipedia.org/wiki/Clovis_culture)

<sup>ii</sup> Hall, M. and L. Gorden. A Knife River Flint Clovis Point from St. Charles County, Missouri.

[http://csasi.org/2005\\_april\\_journal/a\\_knife\\_river\\_flint\\_clovis\\_point\\_from\\_st\\_charles\\_co\\_unty.htm](http://csasi.org/2005_april_journal/a_knife_river_flint_clovis_point_from_st_charles_co_unty.htm)

<sup>iii</sup> [http://en.wikipedia.org/wiki/Clovis\\_point](http://en.wikipedia.org/wiki/Clovis_point)

<sup>iv</sup> Hirst, K. (2008), Clovis, black mats, and extra-terrestrials.

<http://archaeology.about.com/b/2008/04/28/clovis-black-mats-and-extra-terrestrials.htm>

<sup>v</sup> Parks: San Pedro Riparian National Conservation Area - Murray Springs Clovis Site.

[http://gorp.away.com/gorp/resource/us\\_blm/az/arc2\\_san.htm](http://gorp.away.com/gorp/resource/us_blm/az/arc2_san.htm)

<sup>vi</sup> Haynes, C. V. (2008), Younger Dryas "black mats" and the Rancholabrean termination in North America. *PNAS* **108**, 6520-6525.

<sup>vii</sup> Firestone, R. B., et al. (2007), Evidence for an extraterrestrial impact 12,900 years ago that contributed to the megafaunal extinctions and the Younger Dryas cooling. *PNAS* **104**: 16016-16021.

<sup>viii</sup> Surovell, T. A., et al. (2009), An independent evaluation of the Younger Dryas extraterrestrial impact hypothesis. *PNAS* **106**: 18155-18158.

<sup>ix</sup> Kerr, R. A. (2008) Experts find no evidence for a mammoth-killer impact. *Science* **319**: 1331-1332.

<sup>x</sup> Marlon, J. R., et al. (2009) Wildfire responses to abrupt climate change in North America. *PNAS* **106**: 2519-2524.

<sup>xi</sup> Kennett, D. J., et al. (2009) Nanodiamonds in the Younger Dryas boundary layer sediment. *Science* **323**: 94

<sup>xii</sup> Kennet, D. J., et al. (2009) Shock-synthesized hexagonal diamonds in Younger Dryas boundary sediments. *PNAS* **106**: 12623-12628.